Multiphase Flow Journeys-JEM 2015
Campinas-SP, Brazil, March 23-27, 2015

NONLINEAR WAVES AND TRANSFER PROCESSES IN LIQUID FILM FLOW

S. Alekseenko

Institute of Thermophysics,
Novosibirsk State University,
Novosibirsk, Russia

Natural waves on a falling film

Wave evolution

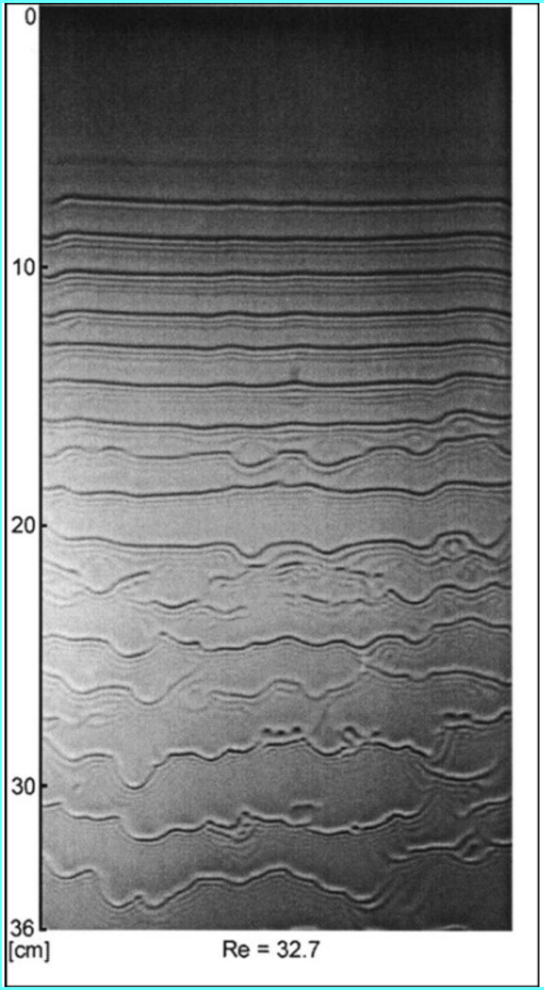

Park, Nosoko: 2003

Waves at a large distance from the inlet: effect of Reynolds number, Re

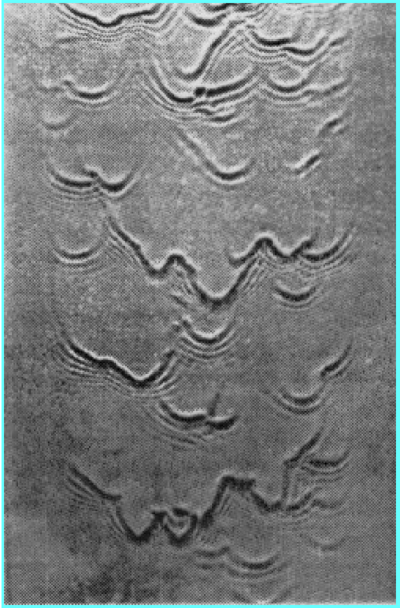

Re = 15

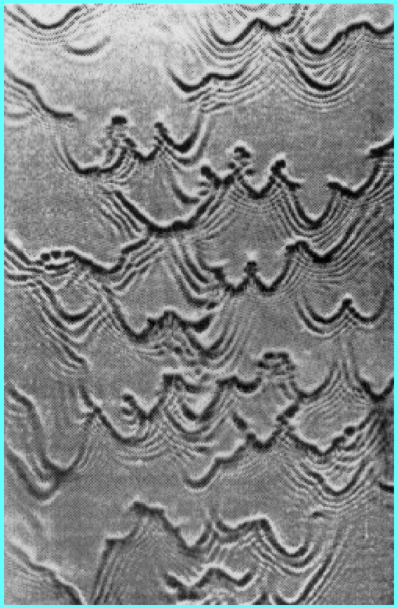

Re = 45

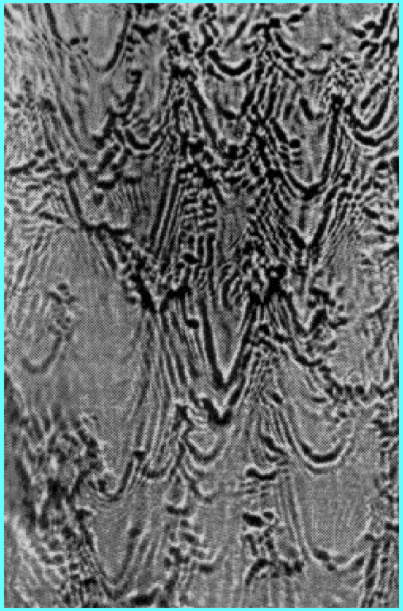

Re = 260

Residual layer: Re < 5

Alekseenko, Nakoryakov, Pokusaev: Wave Flow of Liquid Films, 1994

Wave effect on transfer processes

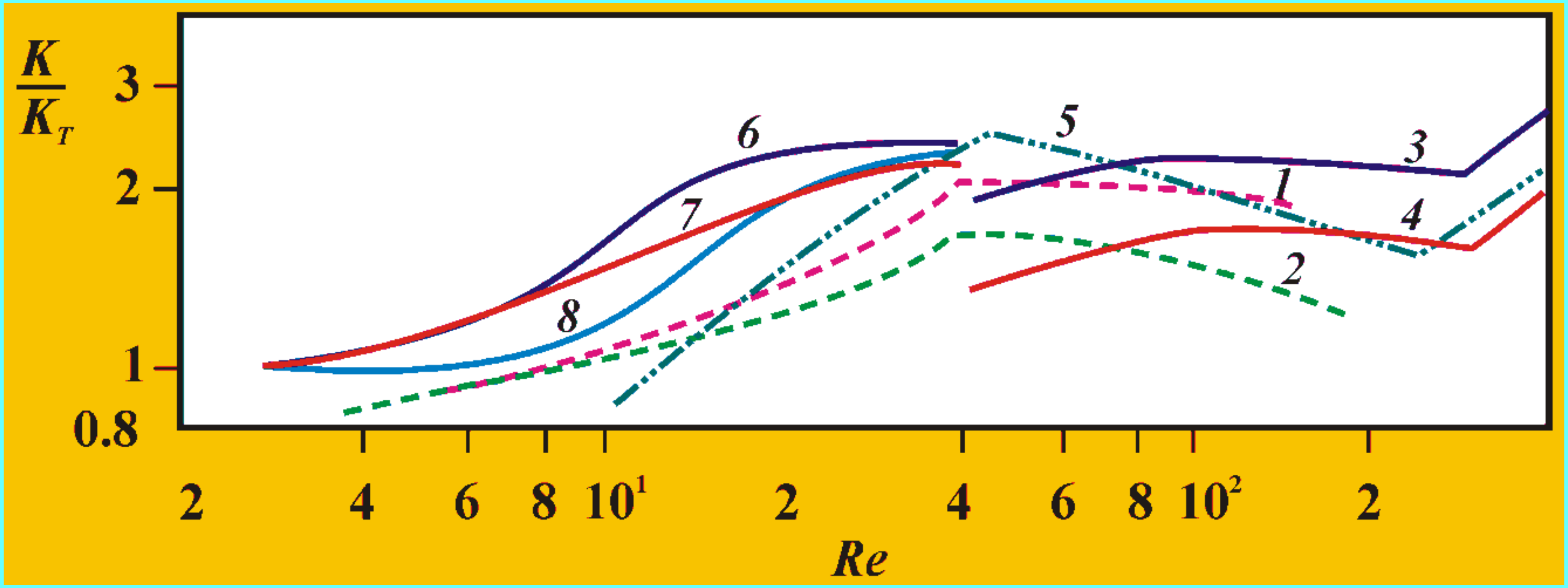

Relative mass transfer coefficient depending on Reynolds number *Re*.
CO_2 absorption by falling liquid film.
K_T - mass transfer in smooth film.
1 – 8 – various experiments

Wave effect up to 170%!

Main regimes of flow with free surface

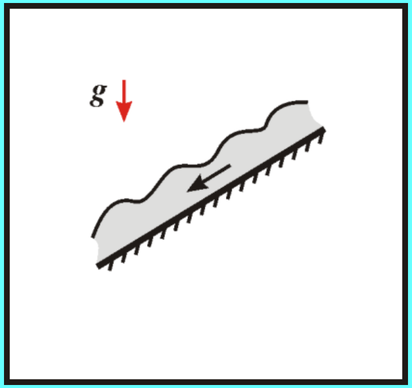

Falling liquid film

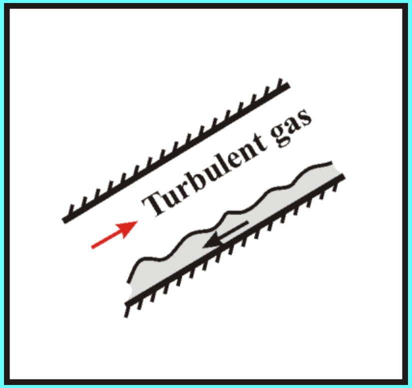

Two-dimensional flow of a liquid film and gas

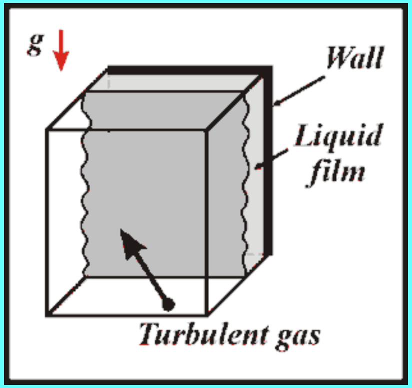

Three-dimensional flow of a liquid film and gas

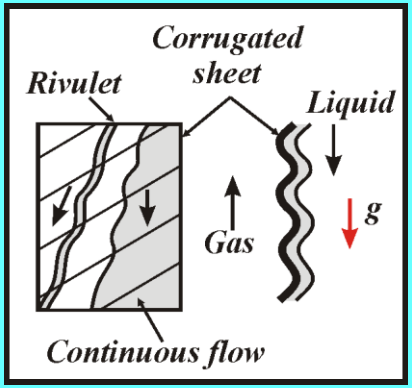

Two-phase flow in regular packing

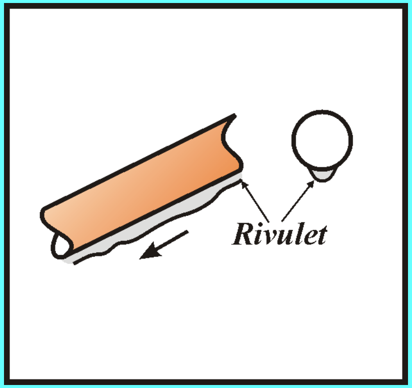

Rivulet on outer side of inclined cylinder

Waves in Brazilian beer BRAHMA Chopp Black

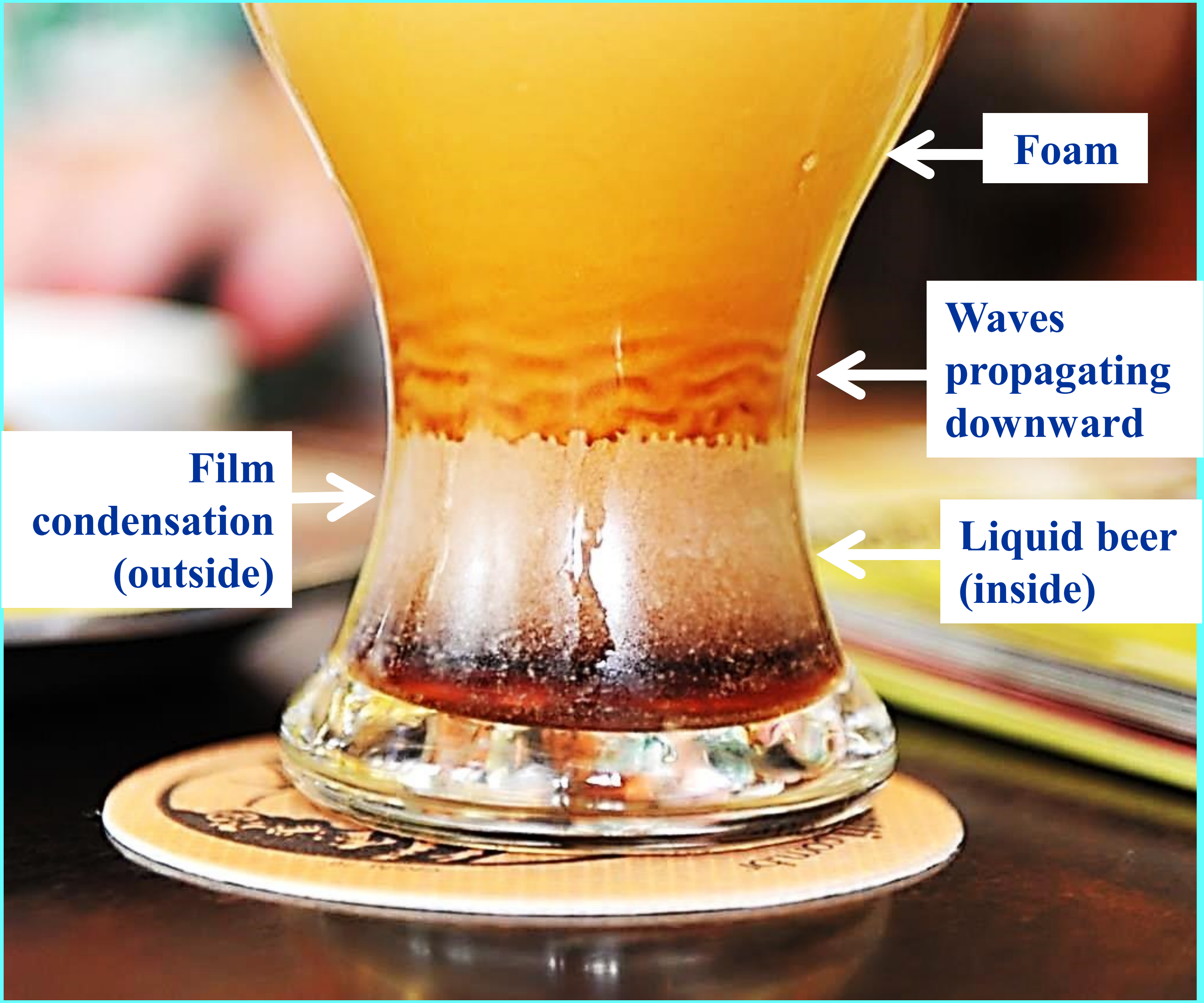

It was observed in Giovannetti bar, Campinas, March 22, 2015

Contents

1. **2-D stationary periodic waves in falling liquid film**
2. **3-D solitary waves in falling liquid film**
3. **Wavy rivulet flow**
4. **Instabilities in annular two-phase flow**
5. **Transport phenomena:**

   Wave effect on condensation and evaporation

1. 2-D STATIONARY PERIODIC WAVES IN FALLING FILM

Two-dimensional stationary waves

Natural waves

Forced waves

Profiles of 2-D forced waves

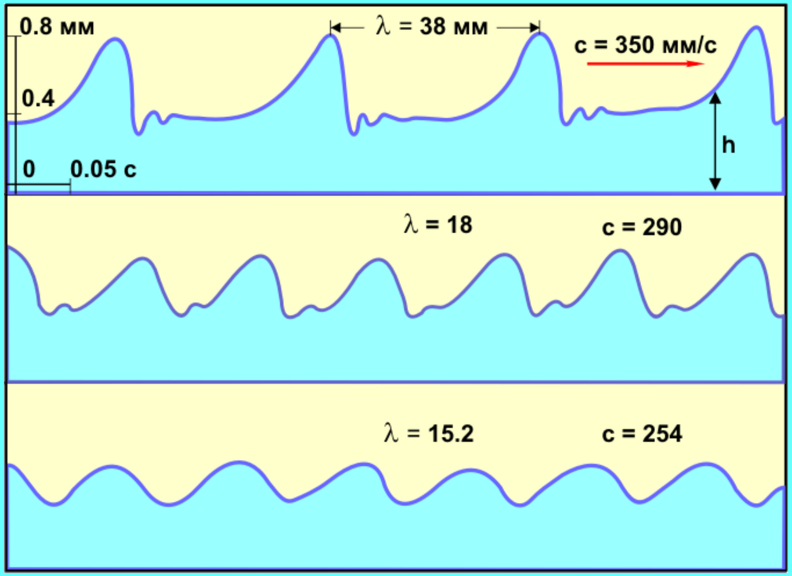

Wave pattern is determined only by forcing frequency

Alekseenko, Nakoryakov, Pokusaev: Wave Flow of Liquid Films, 1994

Two-dimensional stationary waves

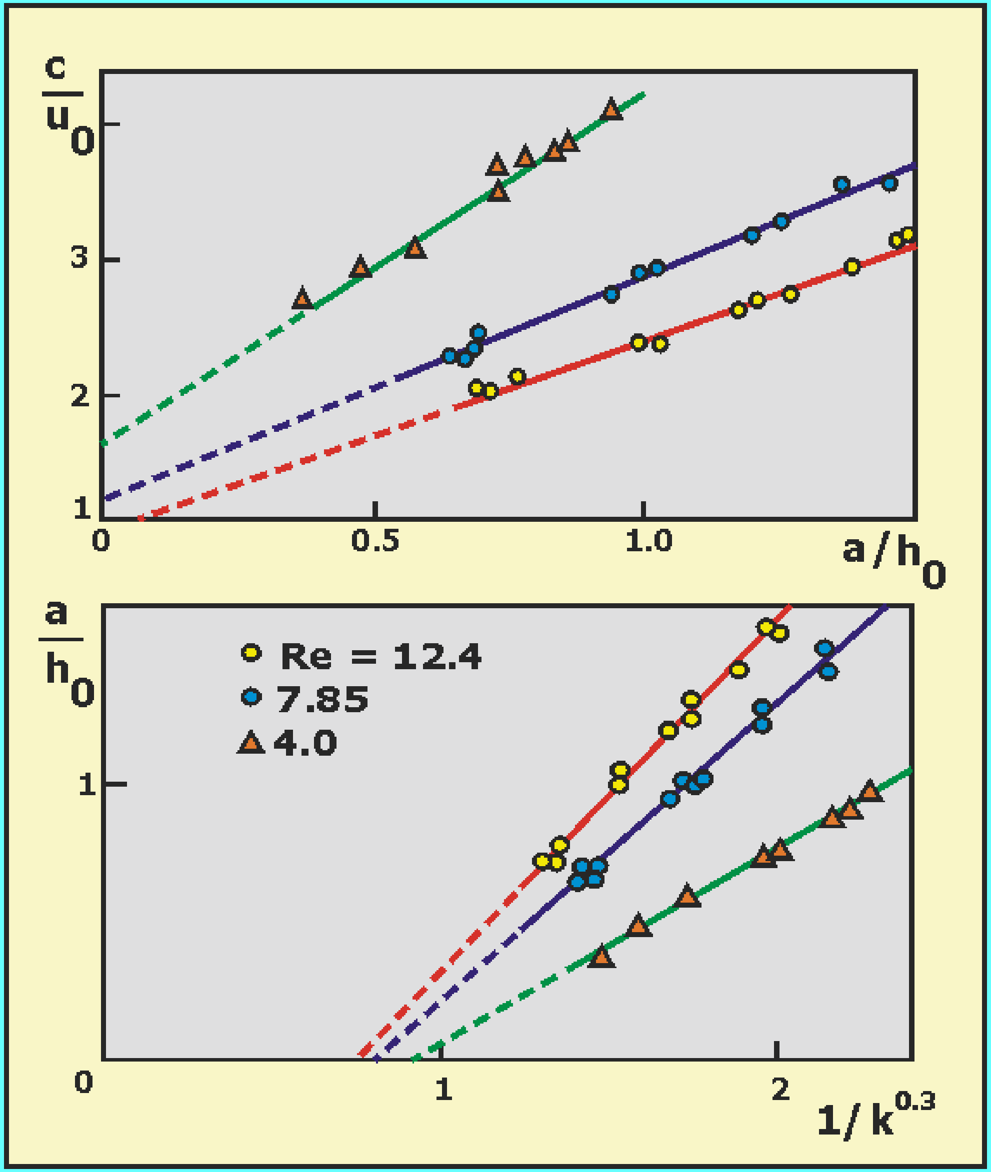

Linear relation between phase velocity *c* and wave amplitude *a* for **nonlinear** stationary waves

Alekseenko, Nakoryakov, Pokusaev: Wave Flow of Liquid Films, 1994

Equations for long 2-D waves at moderate *Re*

Long waves $\varepsilon \ll 1$

Moderate Re: $Re \sim 1/\varepsilon \gg 1,\ W \sim 1/\varepsilon^2 \gg 1.$

Boundary layer approach.
Integral correlation method
(Karman – Pohlhausen method).

Kapitsa (1948),
Shkadov (1967, 1968)

Kinematic condition: $v = \partial h/\partial t + U\,\partial h/\partial x$ at $y = h$

Integrating across a film and supposing $u/U = 2y/h - (y/h)^2$ we obtain

"Integral" equations

$$\frac{\partial q}{\partial t} + \frac{6}{5}\frac{\partial}{\partial x}\left(\frac{q^2}{h}\right) = -\frac{3q}{Re\,h^2} + \frac{3h}{Re} + \frac{3W}{Re}h\frac{\partial^3 h}{\partial x^3},$$

$$\frac{\partial h}{\partial t} + \frac{\partial q}{\partial x} = 0.$$

where $q = \int_0^h u\,dy$

Equations for long 2-D waves at moderate *Re*

Two – wave equation

(Weakly nonlinear and weakly nonstatonary waves)

$$\left(\frac{\partial}{\partial t}+3\frac{\partial}{\partial x}\right)H+\frac{\mathrm{Re}}{3}\left(\frac{\partial}{\partial t}+1.7\frac{\partial}{\partial x}\right)\left(\frac{\partial}{\partial t}+0.7\frac{\partial}{\partial x}\right)H+$$
$$+W\frac{\partial^4 H}{\partial x^4}+6H\frac{\partial H}{\partial x}-\frac{2}{15}\mathrm{Re}\frac{\partial}{\partial t}\left(H\frac{\partial H}{\partial t}\right)=0$$

Limits:

$Re \sim 1$: $\left(\frac{\partial}{\partial t}+c_0\frac{\partial}{\partial x}\right)H=0 \qquad c_0=3$

Kinematic waves
(zero approximation)

$$\frac{\partial \mathrm{H}}{\partial t}+3\frac{\partial \mathrm{H}}{\partial x}+6\mathrm{H}\frac{\partial \mathrm{H}}{\partial x}+\mathrm{Re}\frac{\partial^2 \mathrm{H}}{\partial x^2}+W\frac{\partial^4 \mathrm{H}}{\partial x^4}=0$$

Gjevik's equation
(1-st approximation)

$Re \sim 1/\varepsilon^2 >> 1$: $\left(\frac{\partial}{\partial t}+c_1\frac{\partial}{\partial x}\right)\left(\frac{\partial}{\partial t}+c_2\frac{\partial}{\partial x}\right)H=0.$

Dynamic waves

$c_{1,2}=1.2\pm\sqrt{0.24}\approx 1.69$ and 0.71

Alekseenko, Nakoryakov, Pokusaev: Wave Flow of Liquid Films, 1994

Conclusion

2D stationary nonlinear waves in liquid film flow may be observed under forcing with periodic flow rate pulsations.

Such waves may be adequately described with theoretical models based on the Kapitsa-Shkadov integral approach.

2. 3-D SOLITARY WAVES IN FALLING FILM

Equation for long 3-D waves at *Re* ~ 1

$$\frac{\partial H}{\partial t} + 3\frac{\partial H}{\partial x} + 6H\frac{\partial H}{\partial x} + \boldsymbol{Re}\frac{\partial^2 H}{\partial x^2} + \boldsymbol{W}\left(\frac{\partial^2}{\partial x^2} + \frac{\partial^2}{\partial y^2}\right)^2 \boldsymbol{H} = 0$$

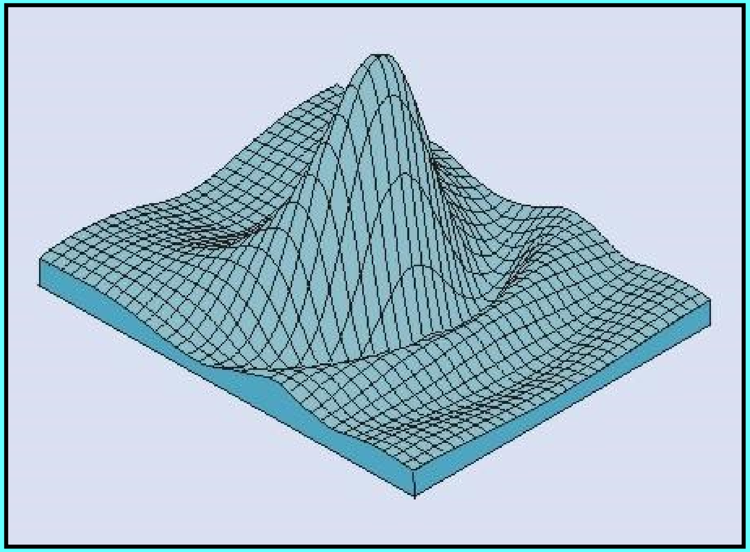

Solitary statinary 3-D wave at *Re* ~ 1
(*Petviashvili, Tsvelodub, 1978*)

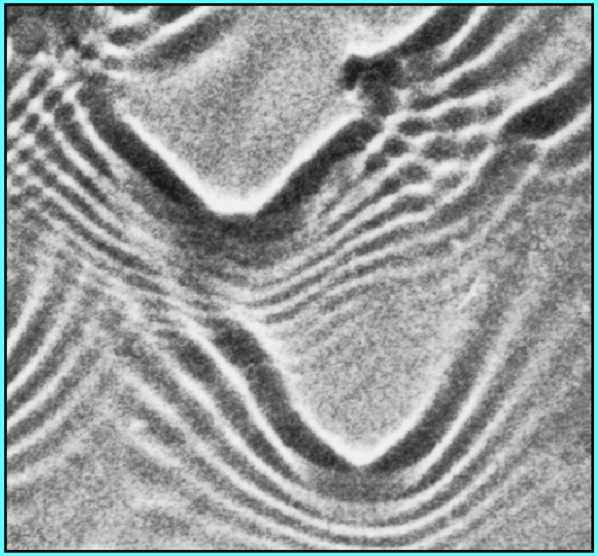

Solitary 3-D wave
(experiment by *Alekseenko et al*)

The three-dimensionality is found only in the capillary term

Equations for long 3-D waves at moderate *Re*

"Integral" equations (*Demekhin, Shkadov, 1984*)

$$
\begin{cases}
h^2\dfrac{\partial q}{\partial t}+\dfrac{6}{5}h\dfrac{\partial q^2}{\partial x}-\dfrac{6}{5}q^2\dfrac{\partial h}{\partial x}+\dfrac{6}{5}h\dfrac{\partial (qm)}{\partial z}- \\
-\dfrac{6}{5}qm\dfrac{\partial h}{\partial z}=h^3\dfrac{3W}{Re}e^2\left(\dfrac{\partial^3 h}{\partial x^3}+\dfrac{\partial^3 h}{\partial z^2\partial x}\right)+ \\
+\dfrac{3h^3}{e\,Re}-\dfrac{3q}{e\,Re}, \\
h^2\dfrac{\partial m}{\partial t}+\dfrac{6}{5}h\dfrac{\partial m^2}{\partial z}-\dfrac{6}{5}m^2\dfrac{\partial h}{\partial z}+\dfrac{6}{5}h\dfrac{\partial (qm)}{\partial x}- \\
-\dfrac{6}{5}qm\dfrac{\partial h}{\partial x}=h^3\dfrac{3W}{Re}e^2\left(\dfrac{\partial^3 h}{\partial z^3}+\dfrac{\partial^3 h}{\partial z\,\partial x^2}\right)-\dfrac{3m}{e\,Re}, \\
\dfrac{\partial h}{\partial t}+\dfrac{\partial q}{\partial x}+\dfrac{\partial m}{\partial z}=0.
\end{cases}
$$

$$q=\int_0^h u\,dy$$

$$m=\int_0^h v\,dy$$

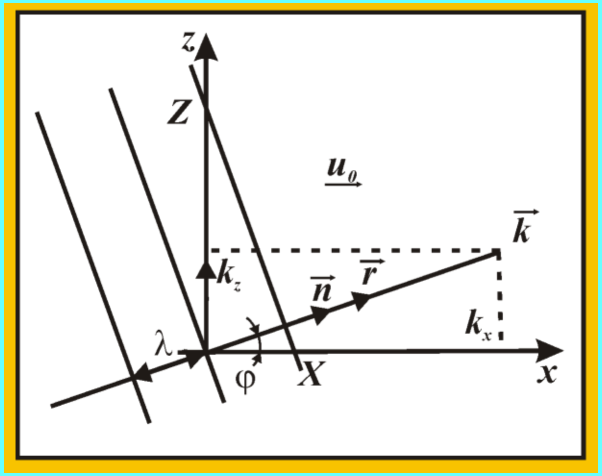

Propagation of elementary plane waves

Limit: Re ~ 1

$$\left(\frac{\partial}{\partial t}+3\frac{\partial}{\partial x}\right)H+6H\frac{\partial H}{\partial x}+Re\frac{\partial^2 H}{\partial x^2}+$$

$$+W\left(\frac{\partial^2}{\partial x^2}+\frac{\partial^2}{\partial z^2}\right)^2 H=0.$$

$$k^2=k_x^2+k_y^2$$

k_n - is neutral wave number for 2D waves

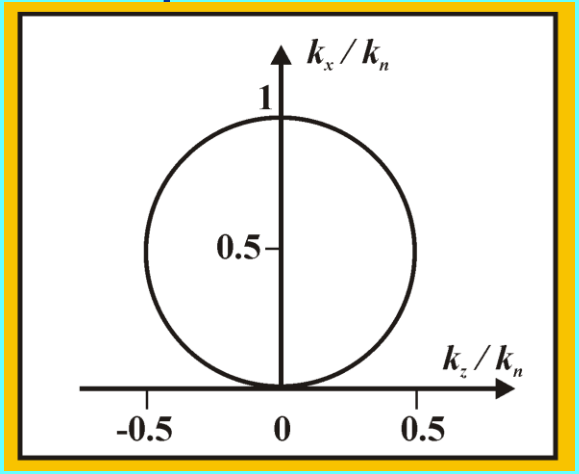

Neutral curve for vertical film flow

Generation of solitary waves

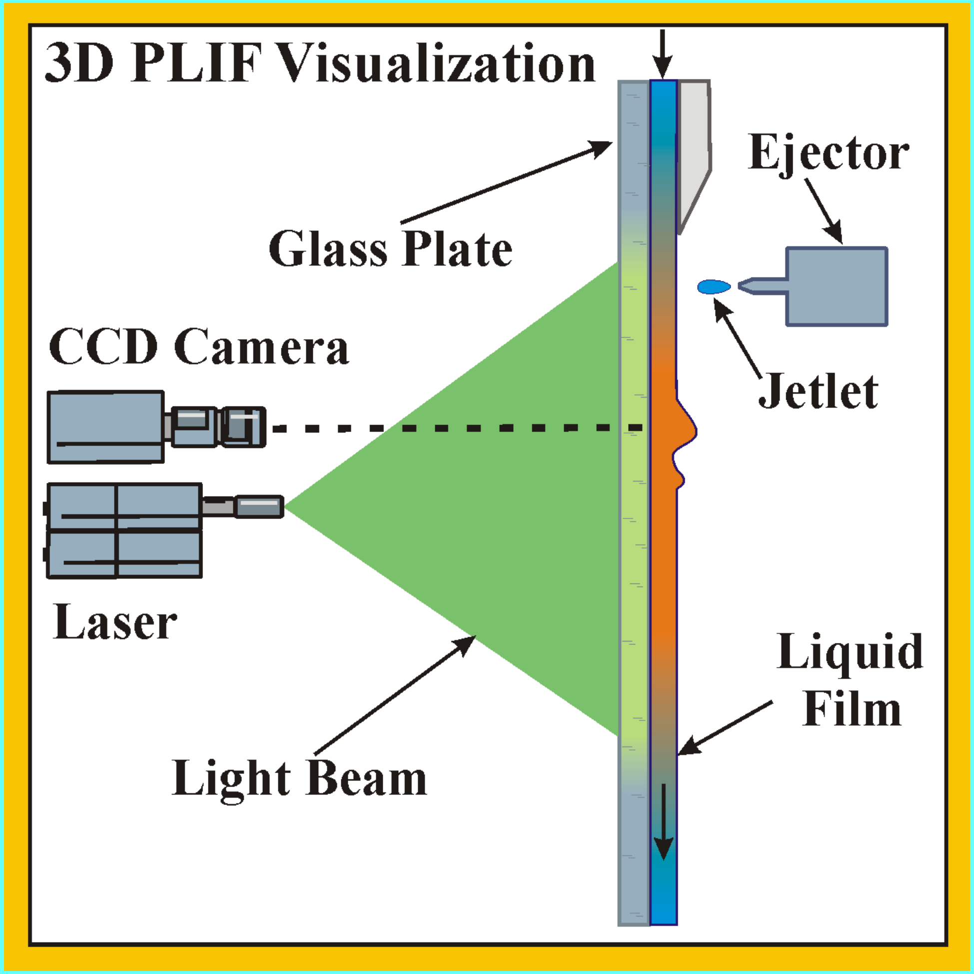

Measurement of 3-D distribution of liquid film thickness with Planar Laser Induced Fluorescence method (PLIF):
Doubled NdYAG Laser (532nm);
CCD Camera "Kodak Megaplus ES1.0" in double frame mode;
Fluorescent dye – Rhodamine 6G , 0.01% wt.

Initial solitary perturbation was produced due to interaction of the jetlet with a smooth film surface.

Alekseenko, Antipin, Guzanov, Markovich, Kharlamov: Phys. Fluids, 2005

Evolution of initial solitary perturbation

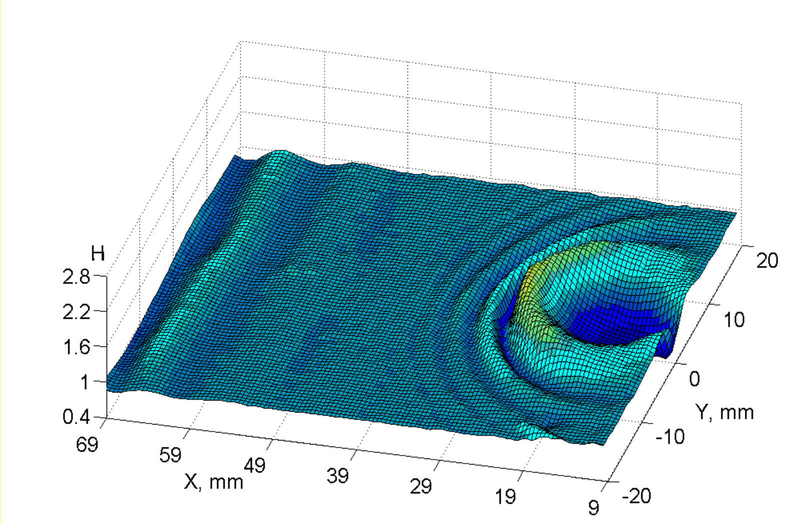

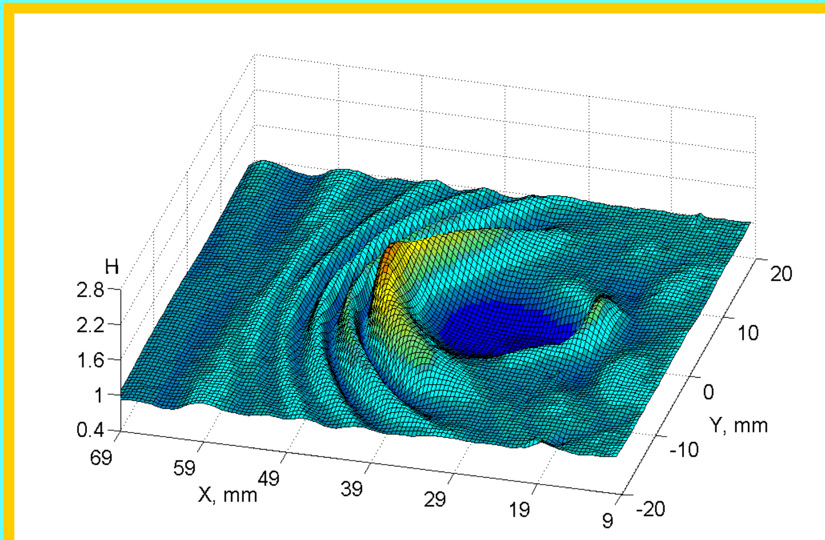

Re = 24.0

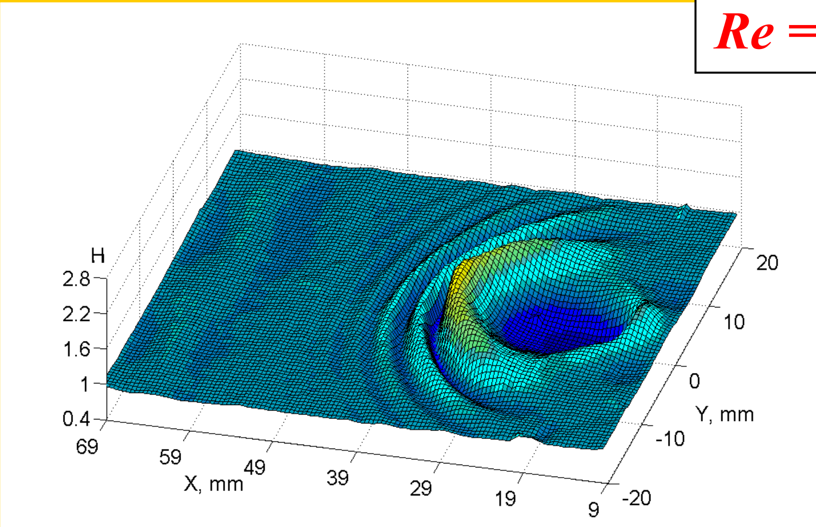

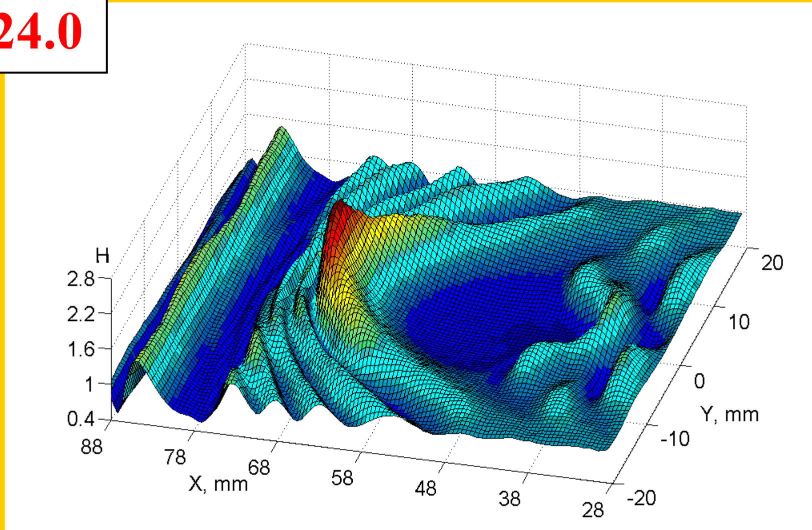

Alekseenko, Antipin, Guzanov, Markovich, Kharlamov: Phys. Fluids, 2005

Shape of 3-D stationary solitary wave

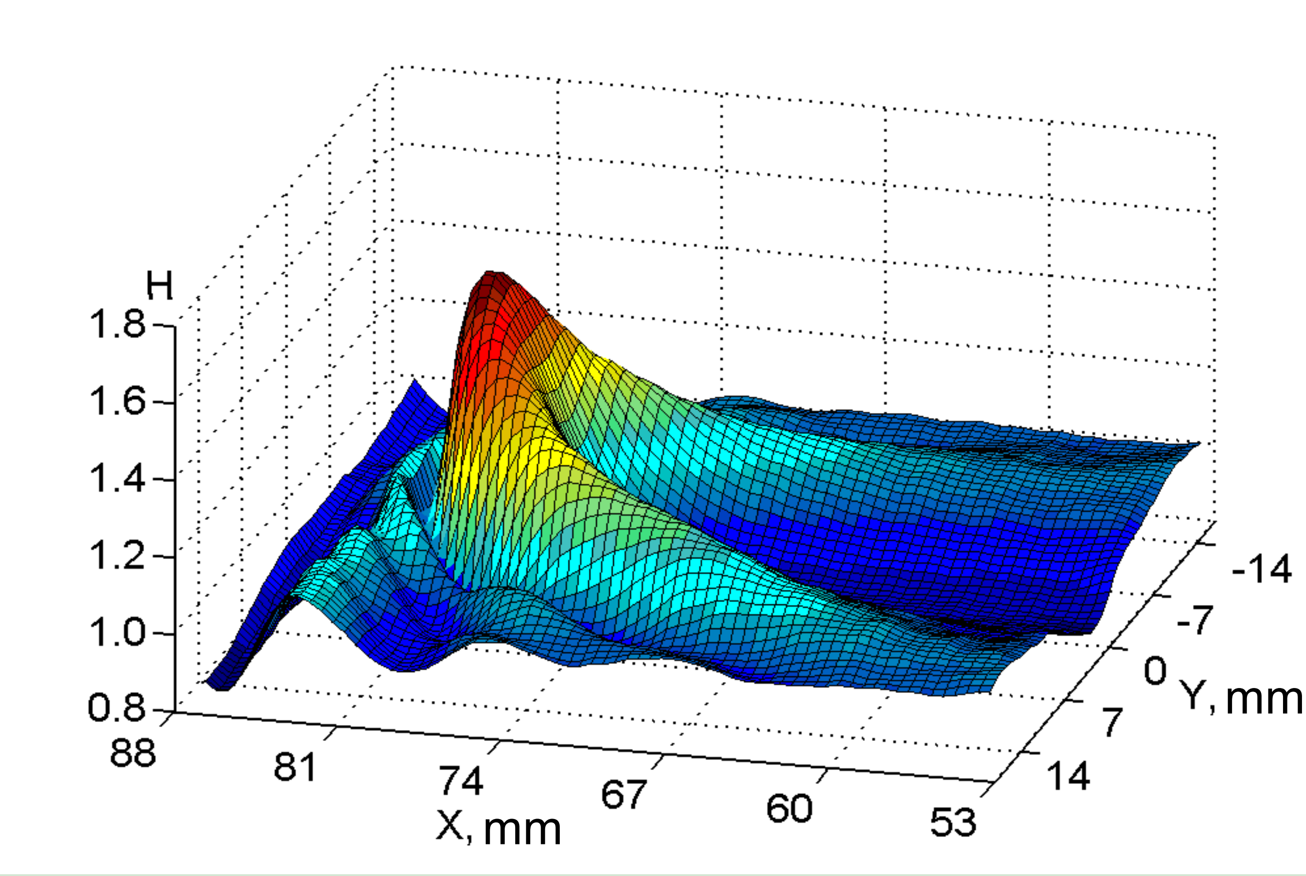

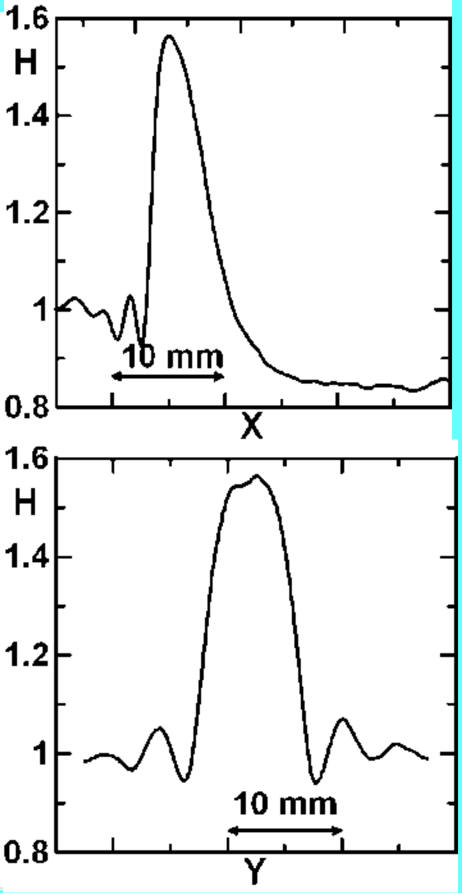

Re = 4.7 (Water-alcohol)

*Alekseenko, Antipin, Guzanov, Markovich, Kharlamov: **Phys. Fluids, 2005***

Shape of 3-D stationary solitary wave

Experiment: Re = 3.9
(Water-alcohol)

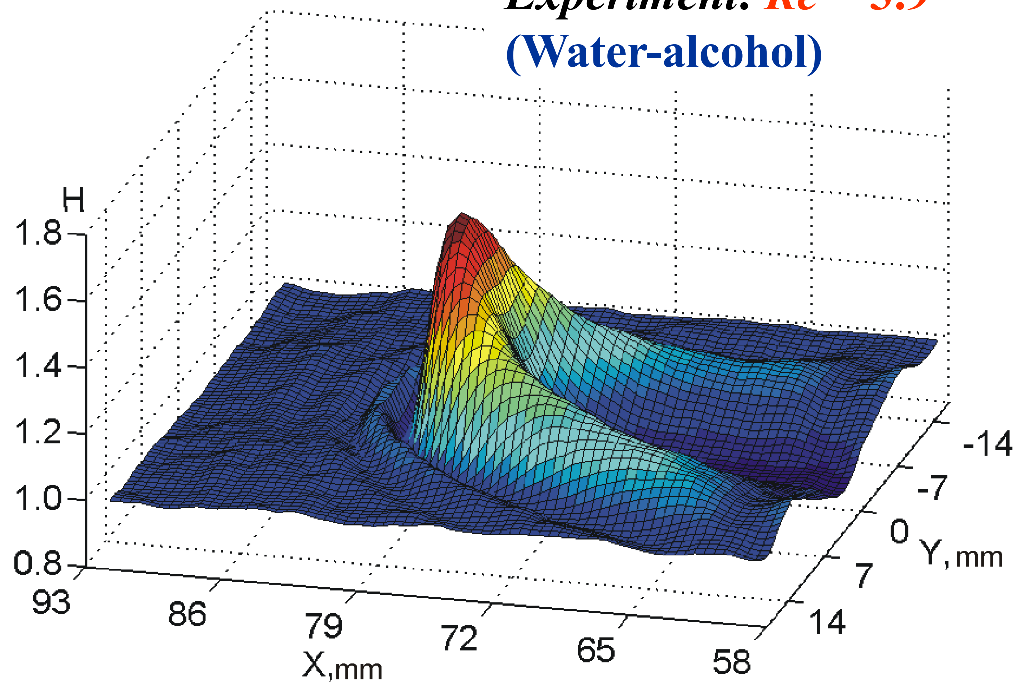

Theory: Demekhin et al (2007)
(Integral equations)

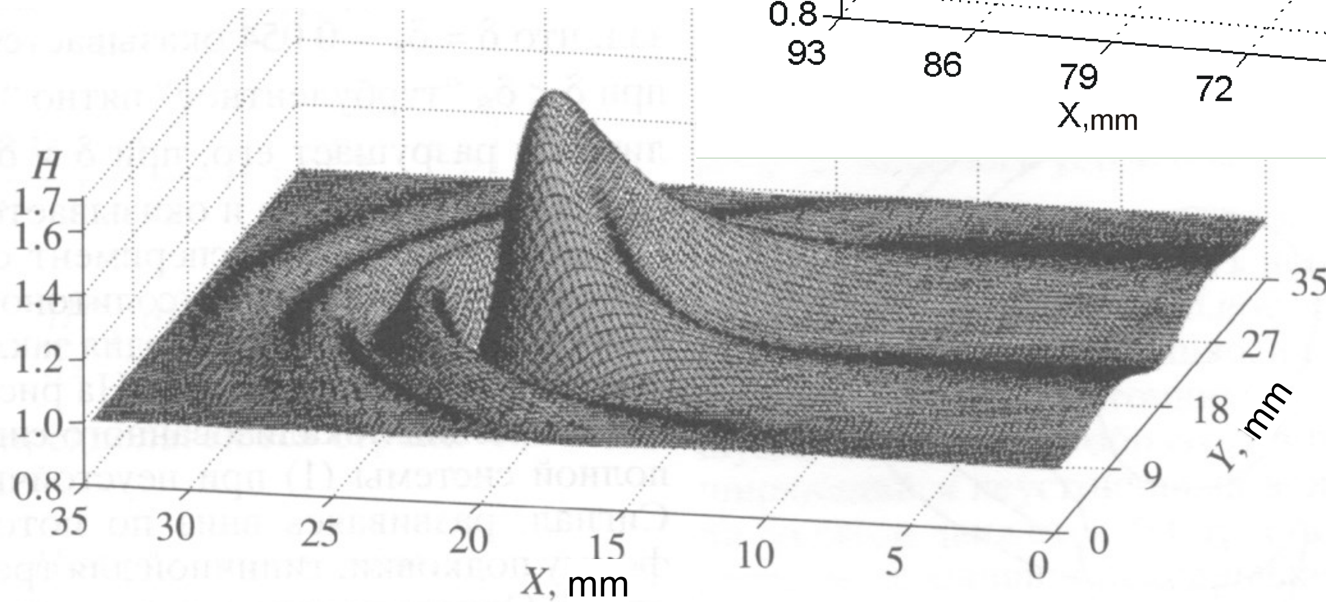

Comparison with theory

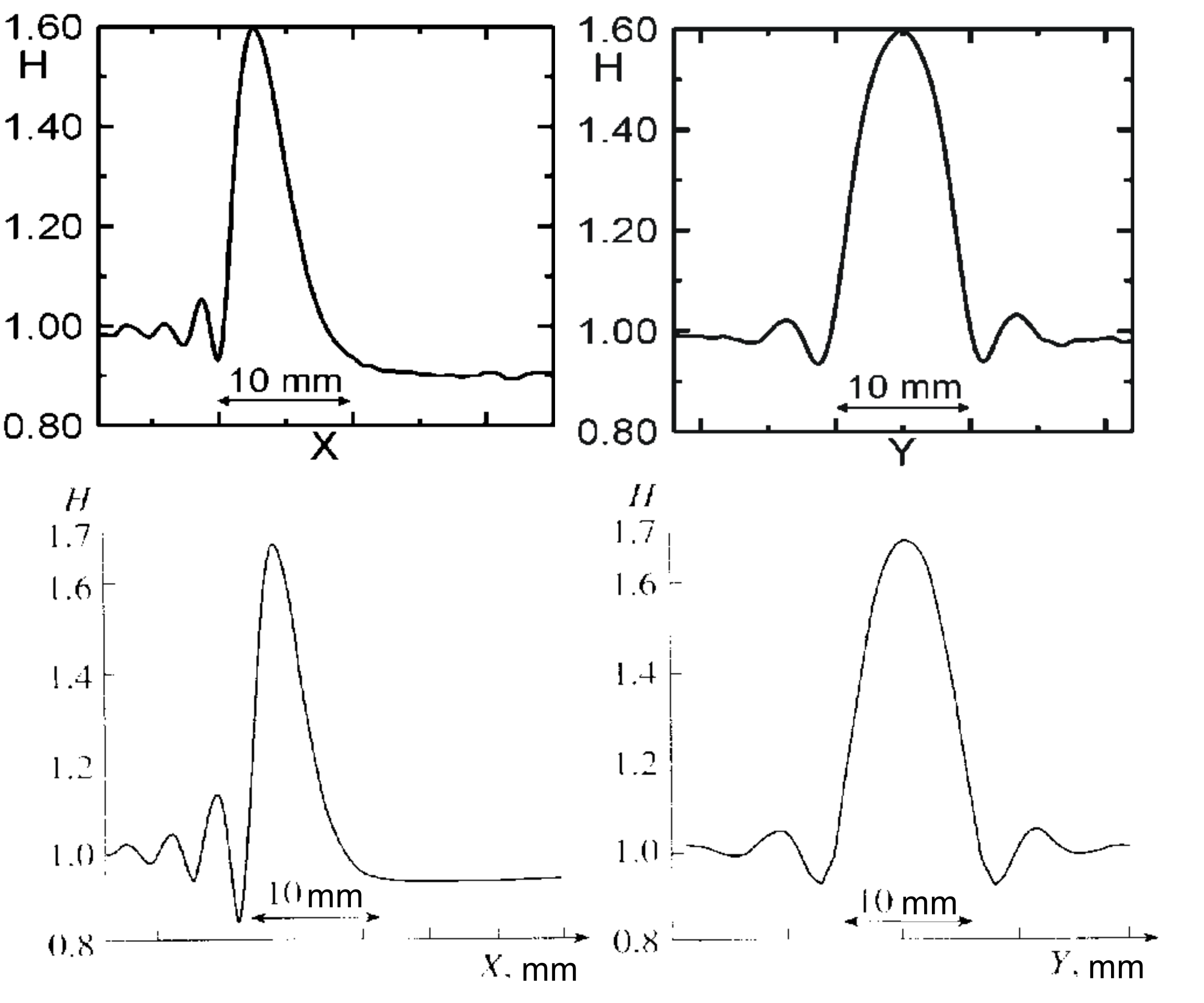

Experiment:
***Re* = 3.9**
(Water-alcohol)

Theory:
Demekhin et al (2007)
(Integral equations)

Double 3-D stationary solitary wave

Experiment:
***Re* = 1.9**

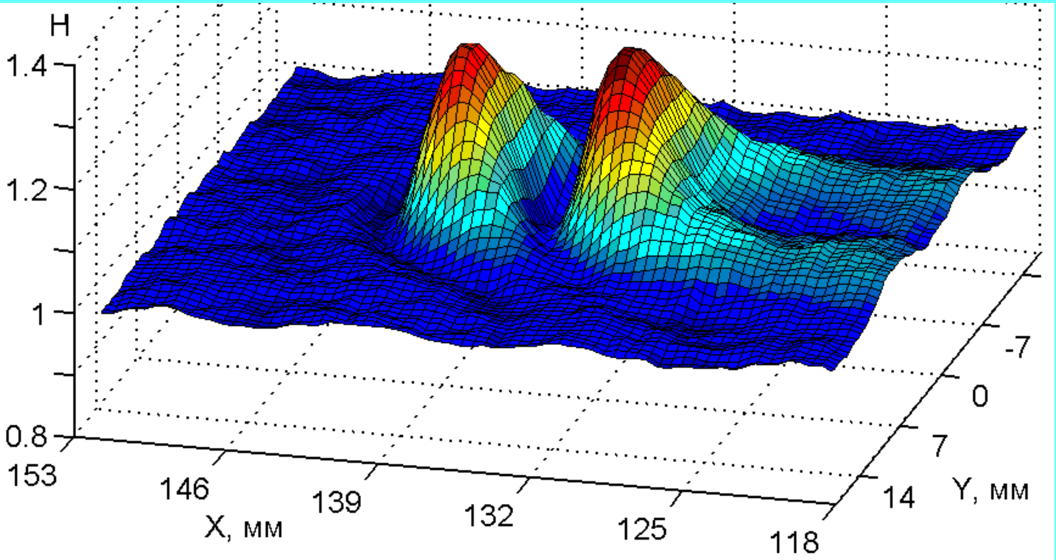

Theory:
Demekhin et al (2007)
(Integral equations)

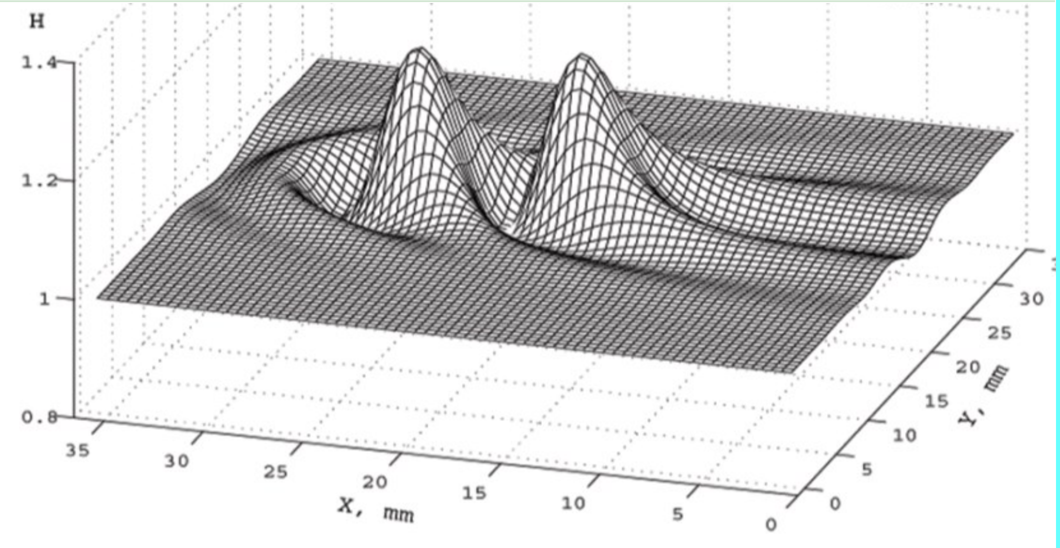

Conclusion

3D stationary solitary waves are found experimentally in liquid film flow. They were predicted previously on the basis of theoretical simulation.

Such type of a wave is considered to be a fundamental element of wavy liquid film flows.

3. WAVY RIVULET FLOW

Rivulets on a solid wall

Rivulet formation at breakdown of the liquid film front

Single rivulet

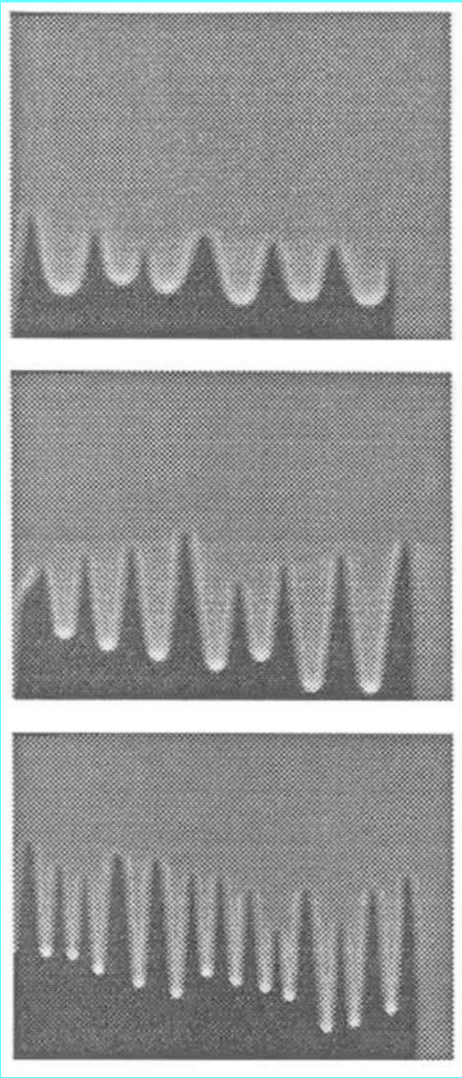

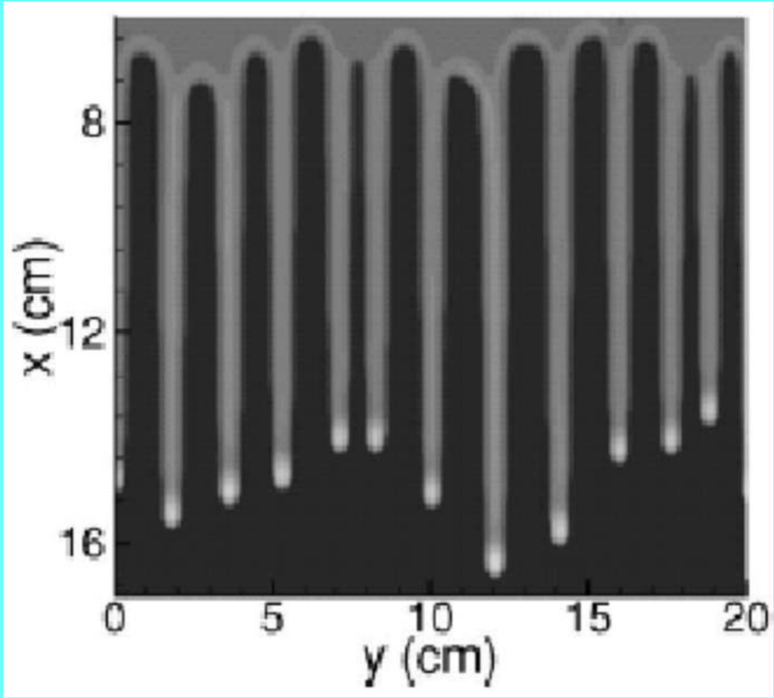

Viscous film flow of water-glycerol solution (Johnson et al. 1999)

Rivulet on inclined cylinder and regular packing

Column for natural gas liquefaction
Air Products and Chemicals (USA)

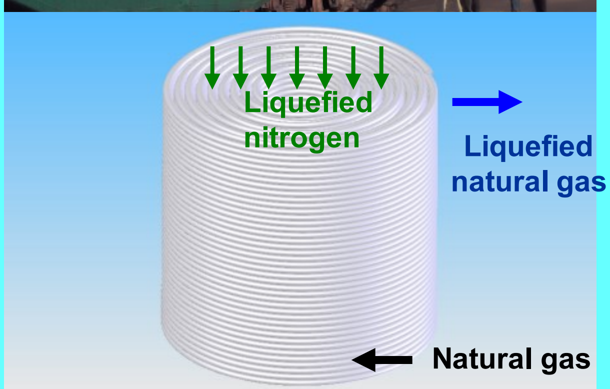

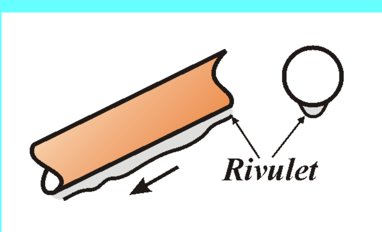

Alekseenko, Markovich,
Shtork: Phys. Fluids, 1996

Two-phase flow in distillation column with regular packing

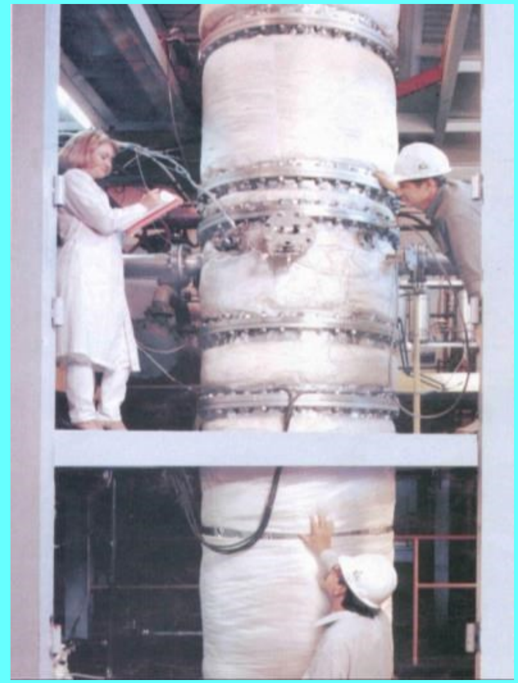

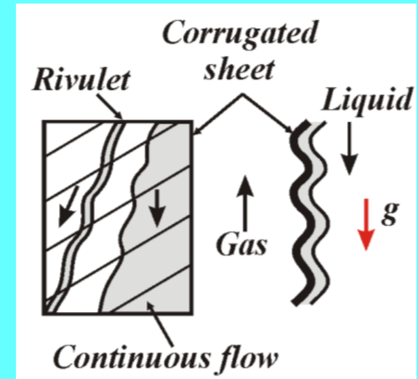

Freon model of distillation column with regular packing (ITP SB RAS)

Alekseenko, Markovich,
Evseev, Bobylev et al:
AIChE J., 2008

Wavy rivulet flow on vertical plate: experiment

Experimental setup and measurement technique

Vertical glass plate or plate with fluoroplastic coating. Plate sizes – 0.2×0.65 m.
Rivulet was formed from slot distributor.

Physical properties of the solutions	Contact angle	Kinematic viscosity, ν, m^2/s	Kinematic surface tension σ/ρ, m^3/s^2
25% water-glycerol solution (WGS)	6 ± 0.2°	$2.4\cdot10^{-6}$	$53.9\cdot10^{-6}$
45% water-ethanol solution (WES)	23 ± 1°	$2.65\cdot10^{-6}$	$32.9\cdot10^{-6}$

Thickness was measured by the Laser-Induced Fluorescence (LIF) method.

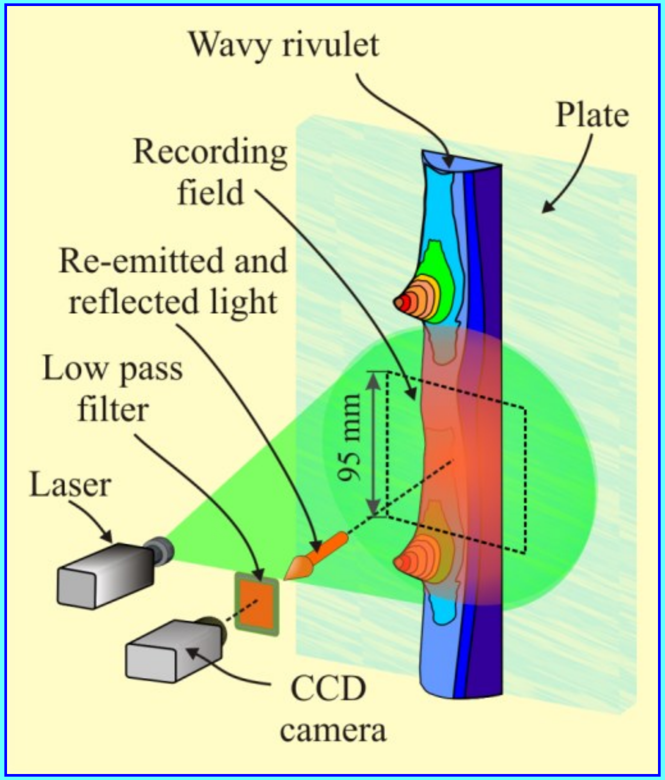

Experimental scheme

Alekseenko, Antipin, Bobylev, Markovich: Berlin, 2009

Wavy rivulet flow on vertical plate: experiment

Regions of existence and wave regimes, α = 6°

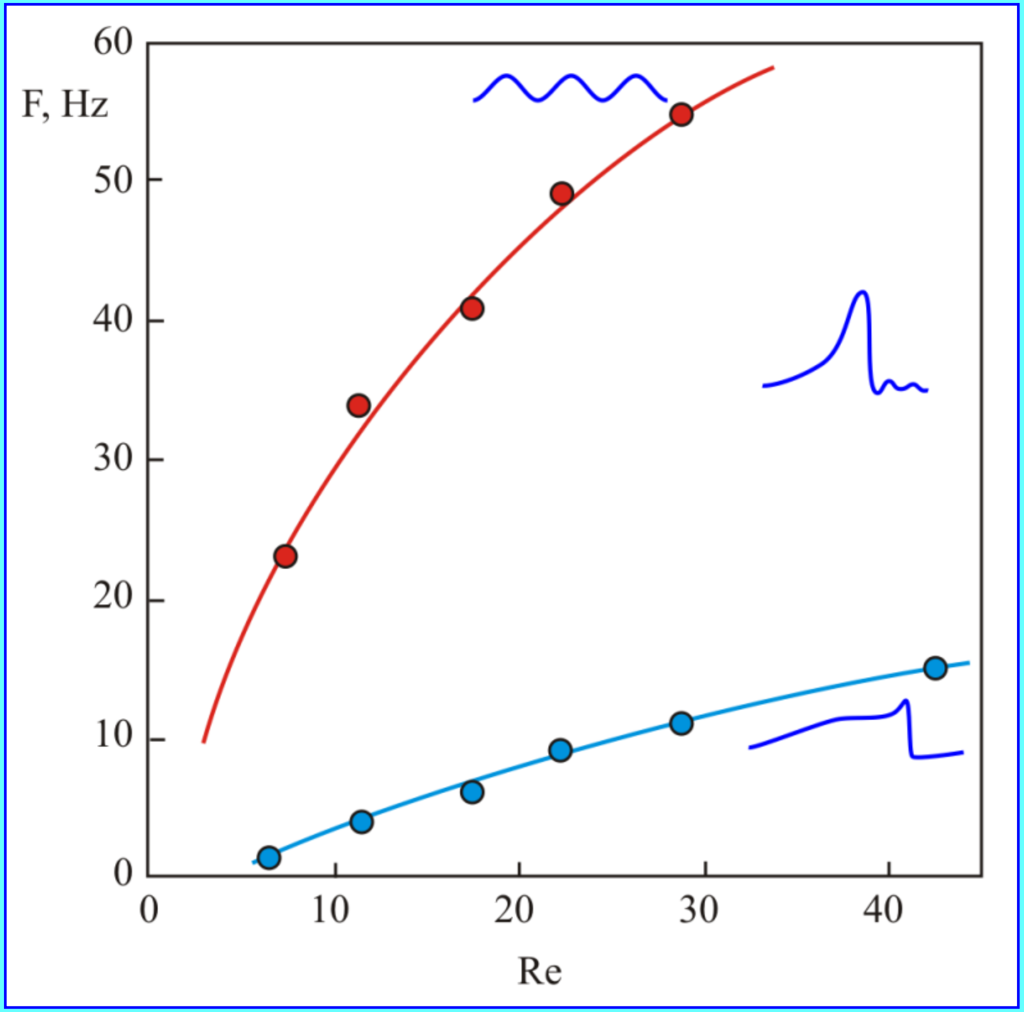

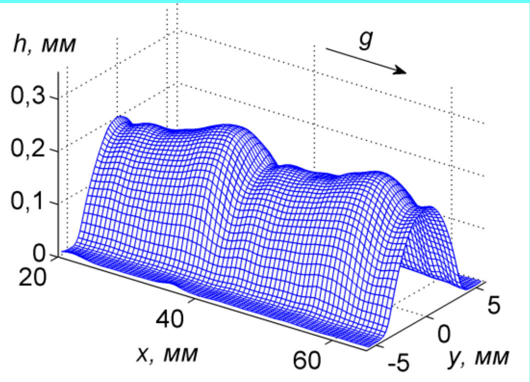

$F = 15$ Hz
$Re = 10$

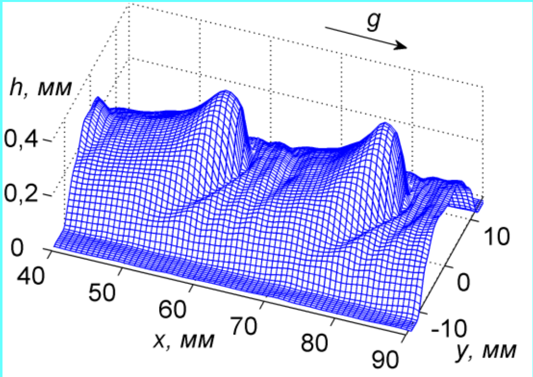

$F = 23$ Hz
$Re = 36$

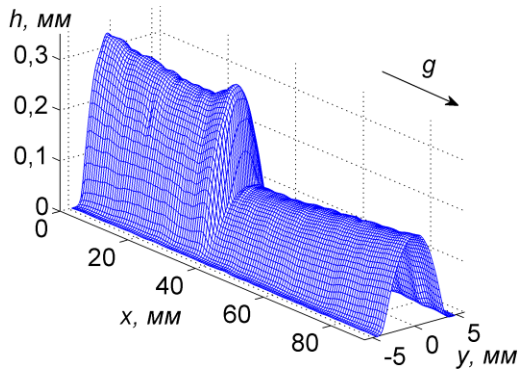

$F = 1$ Hz
$Re = 10$

Wavy rivulet flow on vertical plate: experiment

Profile of rivulet free surface, $\alpha = 6°$.

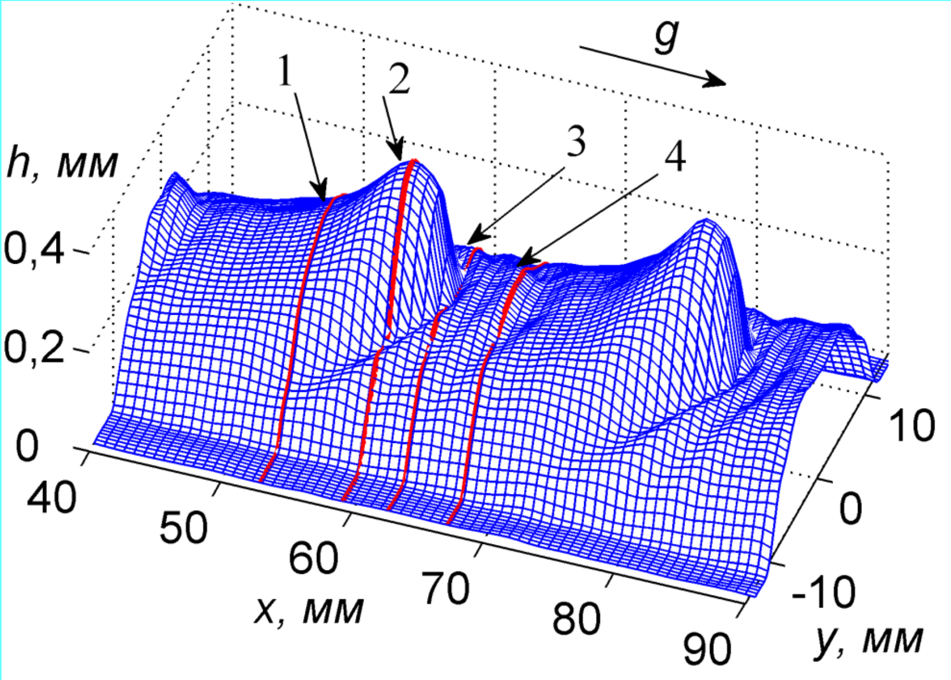

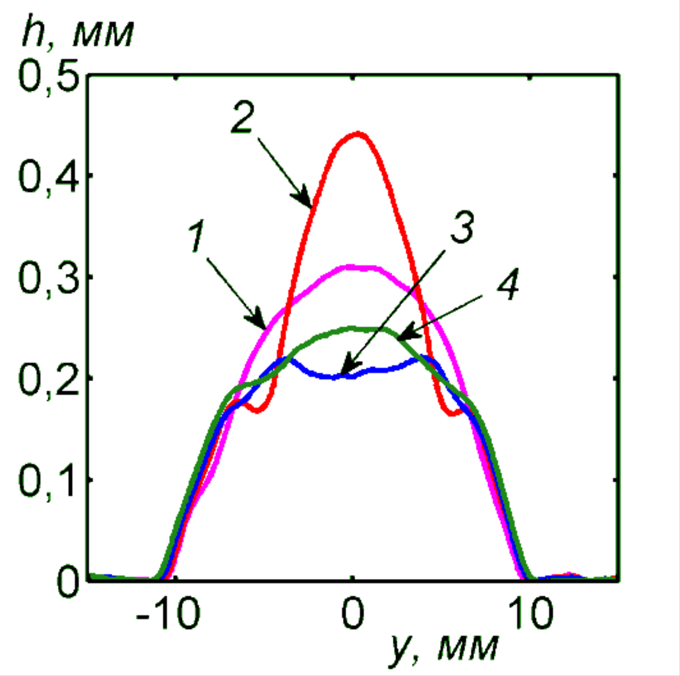

Forcing frequency *F* = 23 Hz; *Re* = 36

Rivulet width is insensitive to the phase of passing wave

Alekseenko et al.: Thermophysics & Aeromech., 2010

Wavy rivulet flow on vertical plate: experiment

Regions of existence and wave regimes, α = 23°

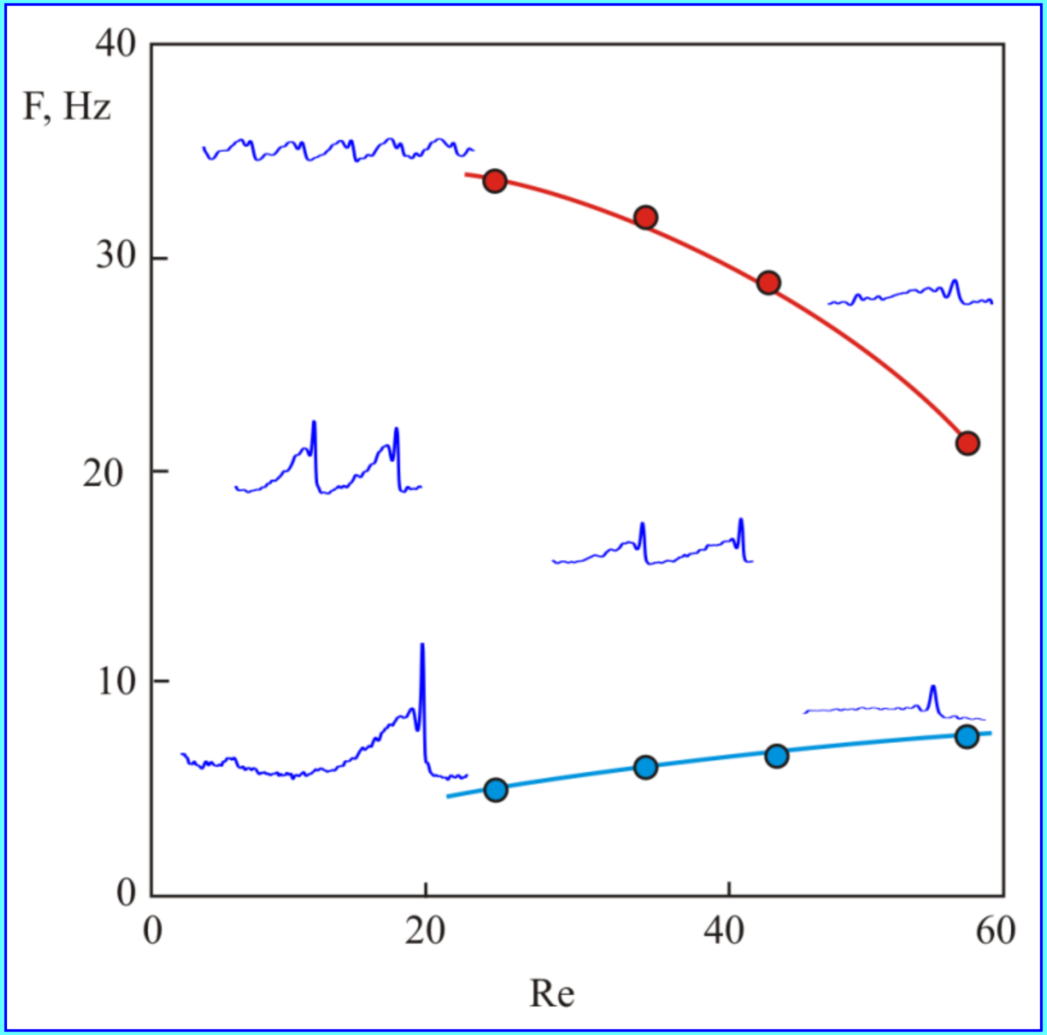

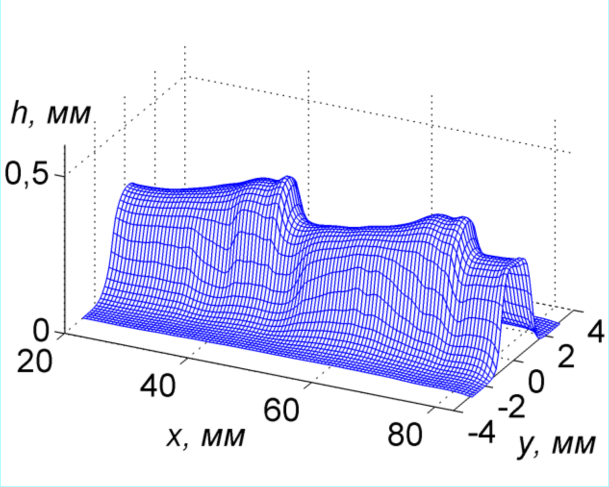

F = 17 Hz, Re = 25

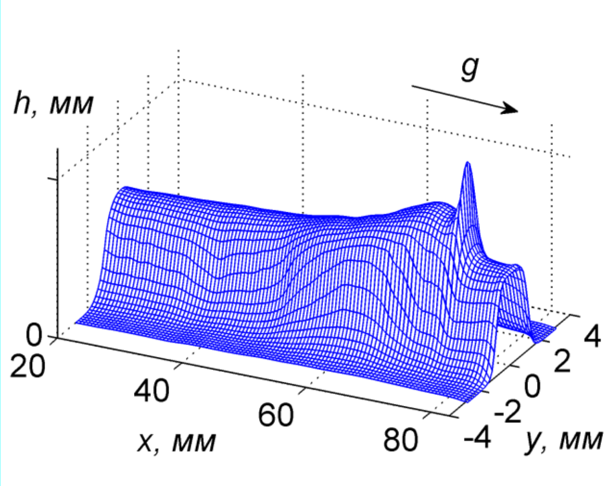

F = 7 Hz, Re = 25

Wavy rivulet flow on vertical plate: theory

Problem statement

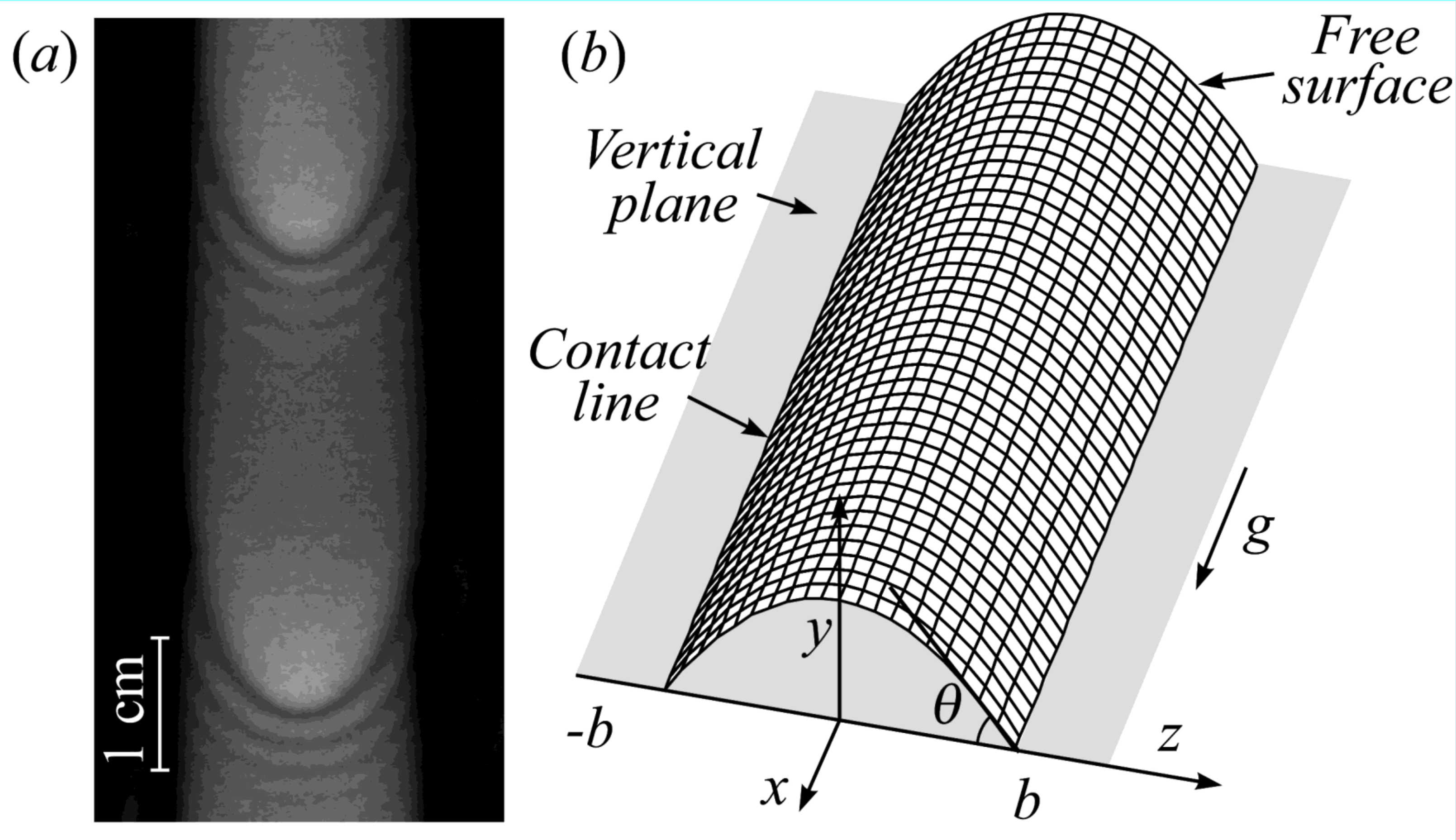

(*a*) Visualization of waves on rivulet surface by the LIF method (experiments of Alekseenko *et al*. (2010), forcing frequency of 17 Hz)
(*b*) Scheme of rivulet flow

Wavy rivulet flow on vertical plate: theory

Thin rivulet: $h \ll b$; long waves: $h \ll \lambda$ ⟶ **Kapitsa-Shkadov integral model.**

Equations of 3D wavy flow of a thin liquid layer (Demekhin & Shkadov 1984):

$$\frac{\partial q}{\partial t}+\frac{6}{5}\left(\frac{\partial}{\partial x}\frac{q^2}{h}+\frac{\partial}{\partial z}\frac{qm}{h}\right)=\frac{3}{Re_m}\left(h-\frac{q}{h^2}\right)+hWe\frac{\partial \Delta h}{\partial x}, \qquad (1)$$

$$\frac{\partial m}{\partial t}+\frac{6}{5}\left(\frac{\partial}{\partial z}\frac{m^2}{h}+\frac{\partial}{\partial x}\frac{qm}{h}\right)=hWe\frac{\partial \Delta h}{\partial z}-\frac{3m}{Re_m\, h^2}, \qquad (2)$$

$$\frac{\partial h}{\partial t}+\frac{\partial q}{\partial x}+\frac{\partial m}{\partial z}=0. \qquad (3)$$

Here $q=\int_0^h u\,dy,\ \ m(x,z,t)=\int_0^h w\,dy$ are flow rates along *Ox* and *Oz* axis, respectively,

h is layer thickness, $\Delta h=\partial^2 h/\partial x^2+\partial^2 h/\partial z^2$ is surface curvature,

$Re_m=gh_0^3/3\nu^2$ is Reynolds number, $We=\left(3Fi/Re_m^5\right)^{1/3}$ is Weber number,

$Fi=\sigma^3/\rho^3 g\nu^4$ is Kapitsa number, σ is surface tension, ρ is density, ν is kinematic viscosity.

Wavy rivulet flow on vertical plate: theory

Boundary conditions for rivulet

Three types of boundary conditions can be defined at the contact line of moving rivulet (Davis 1984):
- **fixed contact line;**
- **fixed contact angle (movable contact line)**
- **movable contact line, subject to existence of a relation between contact angle and velocity of contact line.**

Here we use the boundary conditions of constant contact line (or constant rivulet width), determined in authors' experiments, as well as standard conditions of liquid non-slipping on a solid wall, and symmetry conditions:

$$h(x,b,t)=q(x,b,t)=m(x,b,t)=0, \quad m\big|_{z=0}=0, \quad \partial h/\partial z\big|_{z=0}=\partial q/\partial z\big|_{z=0}=0$$

For stationary rivulet (no waves) solutions to equations (1) - (3) take a form:

$$h=h_{st}=1-z^2/b^2, \qquad q=q_{st}=h_{st}^3(z), \qquad m=0. \qquad \theta_0=arctg(2h_0/b)\approx 2h_0/b$$

Wavy rivulet flow on vertical plate: theory

Numerical simulation of waves in rivulet

Wavy regimes of rivulet flow were obtained through numerical solution of equations (1) – (3) by finite-difference method. Numerical algorithm used the conditions on contact line and conditions of symmetry. Waves were generated at the inlet of calculation domain, where flow rate fluctuations were set:

$$q(0,z,t)=q_{st}\left(1+A_Q\sin 2\pi ft\right).$$

;

Here A_Q is amplitude, f is given forcing frequency

Initial conditions:

$$h(x,0)=h_{st}(x),$$

$$q(x,0)=q_{st}(x).$$

Alekseenko, Aktershev, Bobylev, Kharlamov, Markovich:
J. Fluid Mech., 2015 (in press)

Wavy rivulet flow on vertical plate: theory

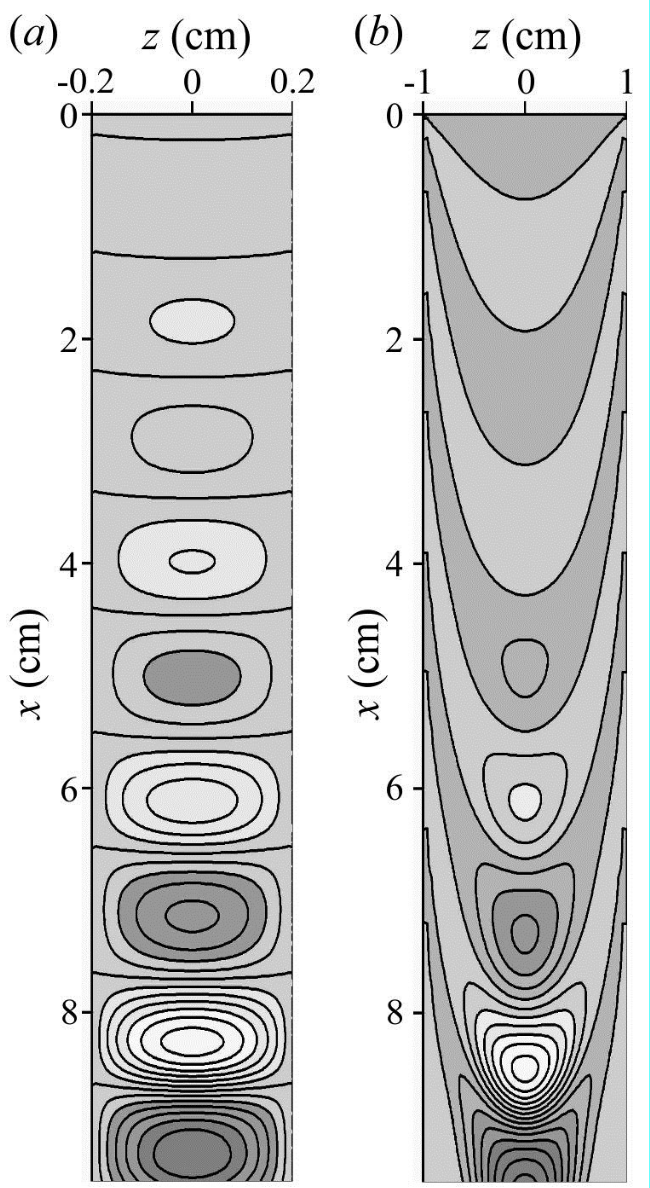

WES WGS

Evolution of linear perturbations

Flow rate pulsations at the inlet:

$$q(0,z,t) = q_{st}(1 + A_Q \sin 2\pi ft).$$

Perturbation of rivulet surface $\delta h = h(x,z,t) - h_{st}(z)$ **is shown in the form of isolines** $\delta h = const$ **at** $f = 15$ **Hz,** $A_Q = 0.01$**,** $Re_m = 25$**.**

For WES rivulet perturbations are almost two-dimensional, while for WGS rivulet they are essentially three-dimensional.

Development of linear perturbations is accompanied by exponential growth (or attenuation) of amplitude with distance.

Dispersion dependencies for linear perturbations at $Re_m = 25$; WES

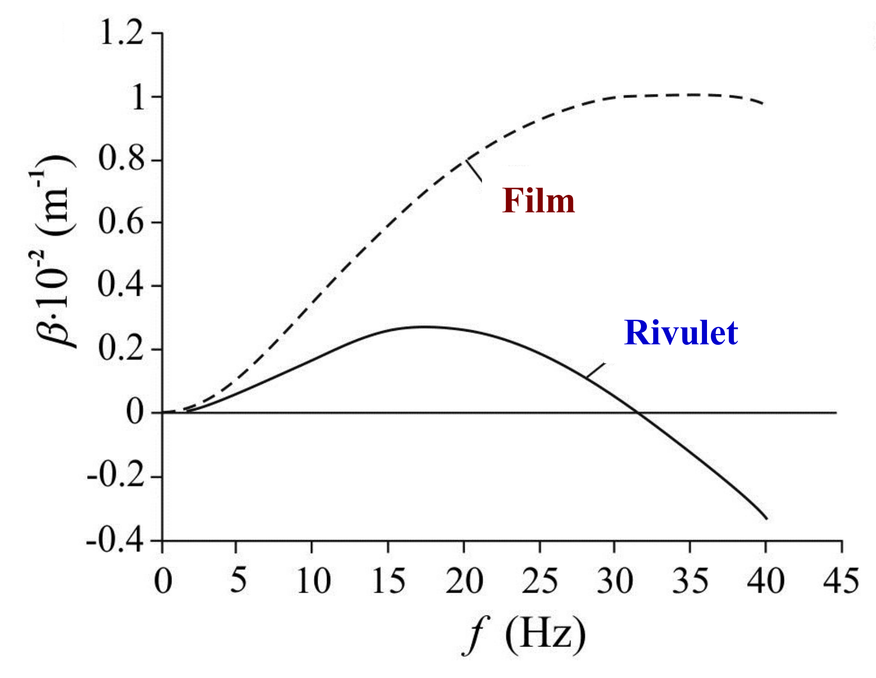

Increment *β* versus forcing frequency *f*

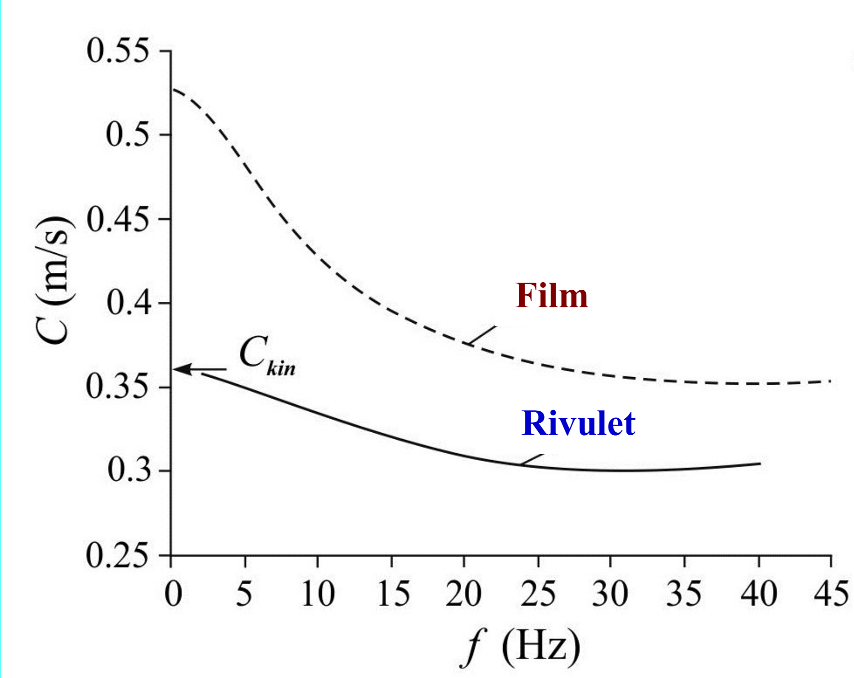

Phase speed *C* versus forcing frequency *f*

Solid lines present 3D perturbations of rivulet surface. Dashed lines are corresponding dependences for 2D waves in the film, calculated by linear theory.

Wavy rivulet flow on vertical plate: theory

Evolution of 3D nonlinear waves at $Re_m = 25$ for different forcing frequencies

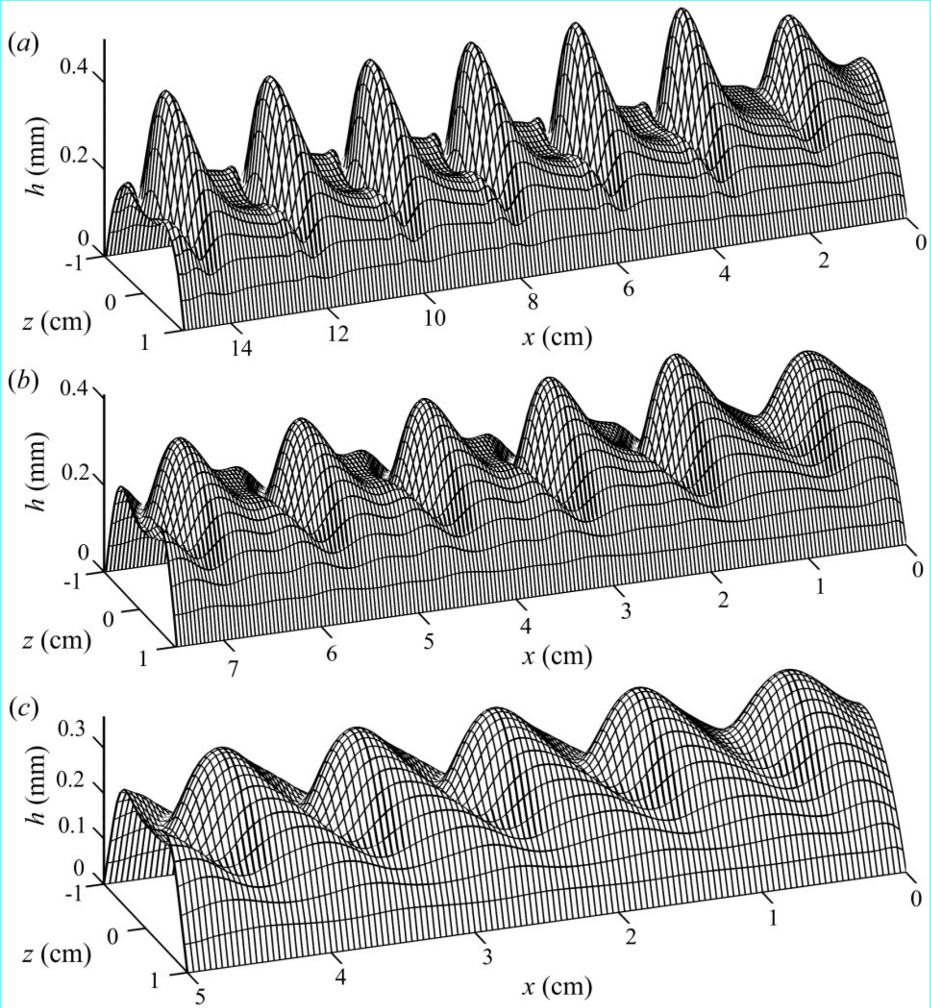

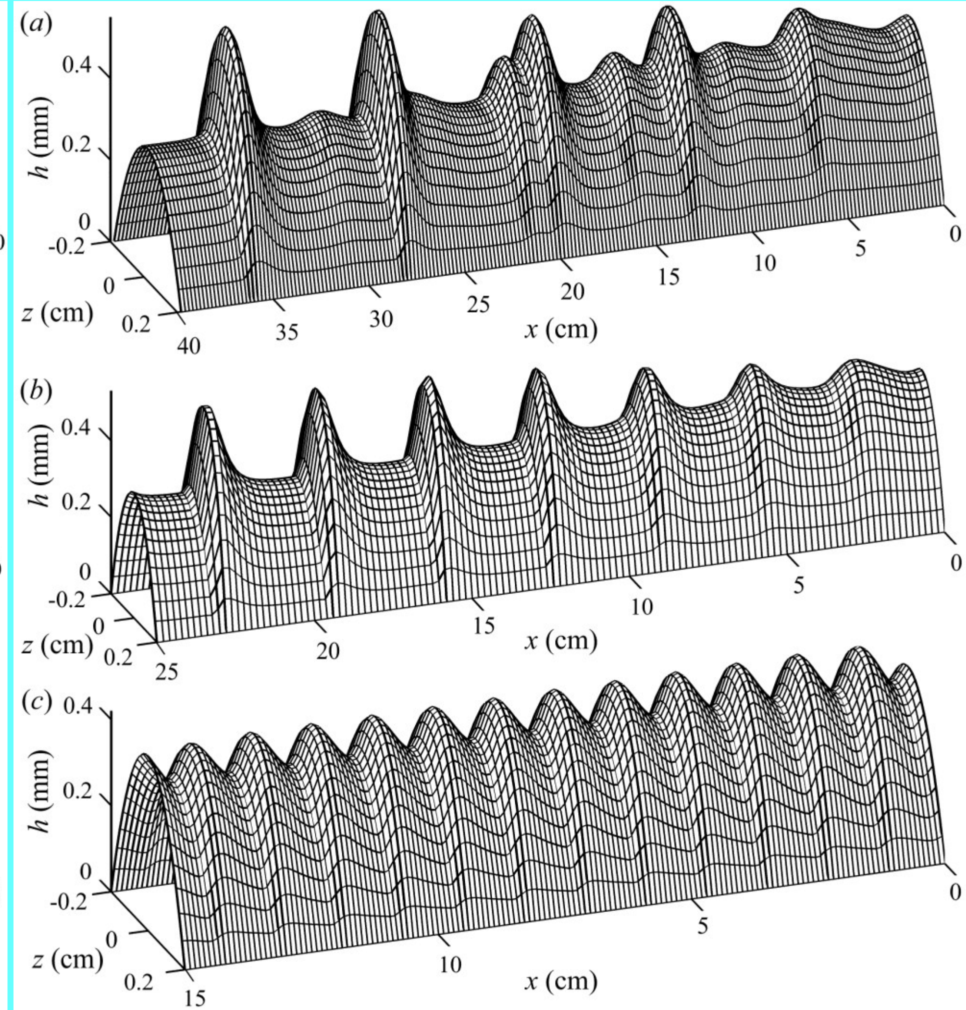

WGS: (*a*) 15 Hz, (*b*) 23Hz, (*c*) 30 Hz

WES: (*a*) 5 Hz, (*b*) 10 Hz, (*c*) 25 Hz

Wavy rivulet flow on vertical plate: theory

Developed nonlinear waves: comparison with experiment

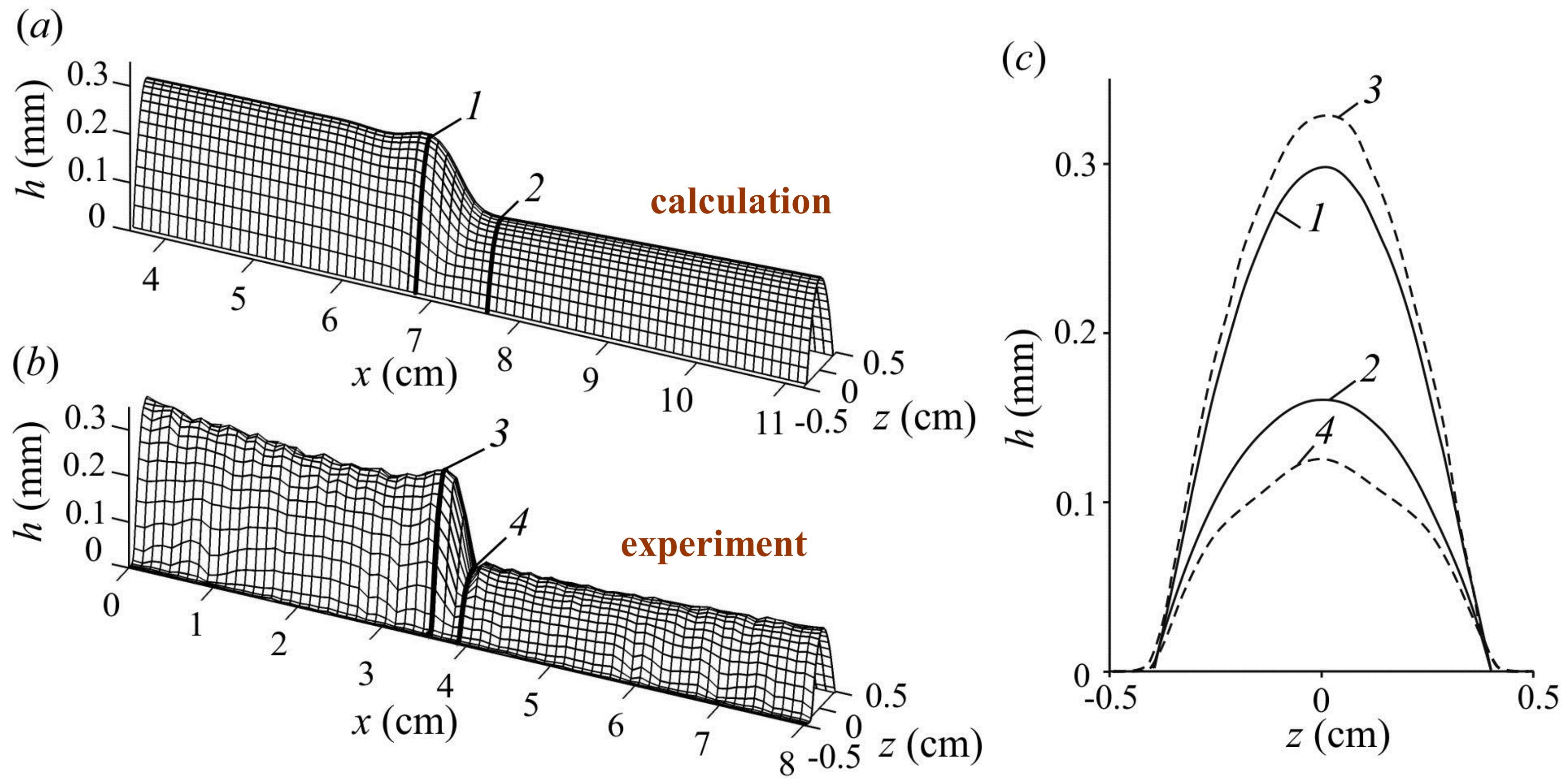

Shape of low-frequency wave in WGS rivulet compared to the experimental data (Alekseenko *et al*. 2010) at $Re_m = 10$, $f = 1$ Hz.
(*a*) calculated 3D surface, (*b*) experimental 3D surface,
(*c*) cross-sections: (1, 2) calculation, (3, 4) experiment.

Wavy rivulet flow on vertical plate: theory

Developed nonlinear waves: comparison with experiment

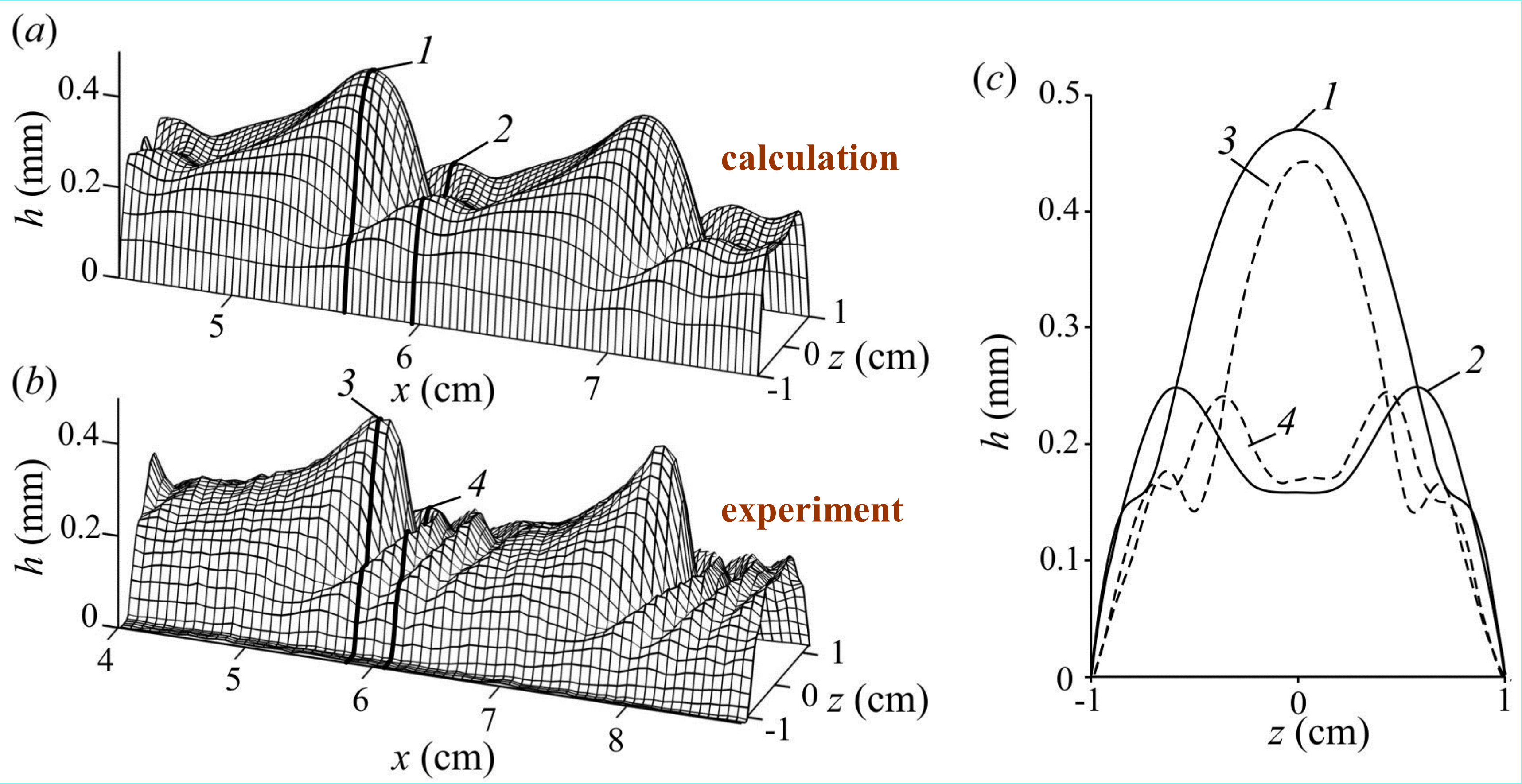

Shape of developed wave in WGS rivulet compared to the experimental data (Alekseenko *et al*. 2010) at $Re_m = 36$, $f = 23$ Hz.
(*a*) calculated 3D surface, (*b*) experimental 3D surface,
(*c*) cross-sections: (1, 2) calculation, (3, 4) experiment.

Wavy rivulet flow on vertical plate: theory

Developed nonlinear waves: comparison with experiment

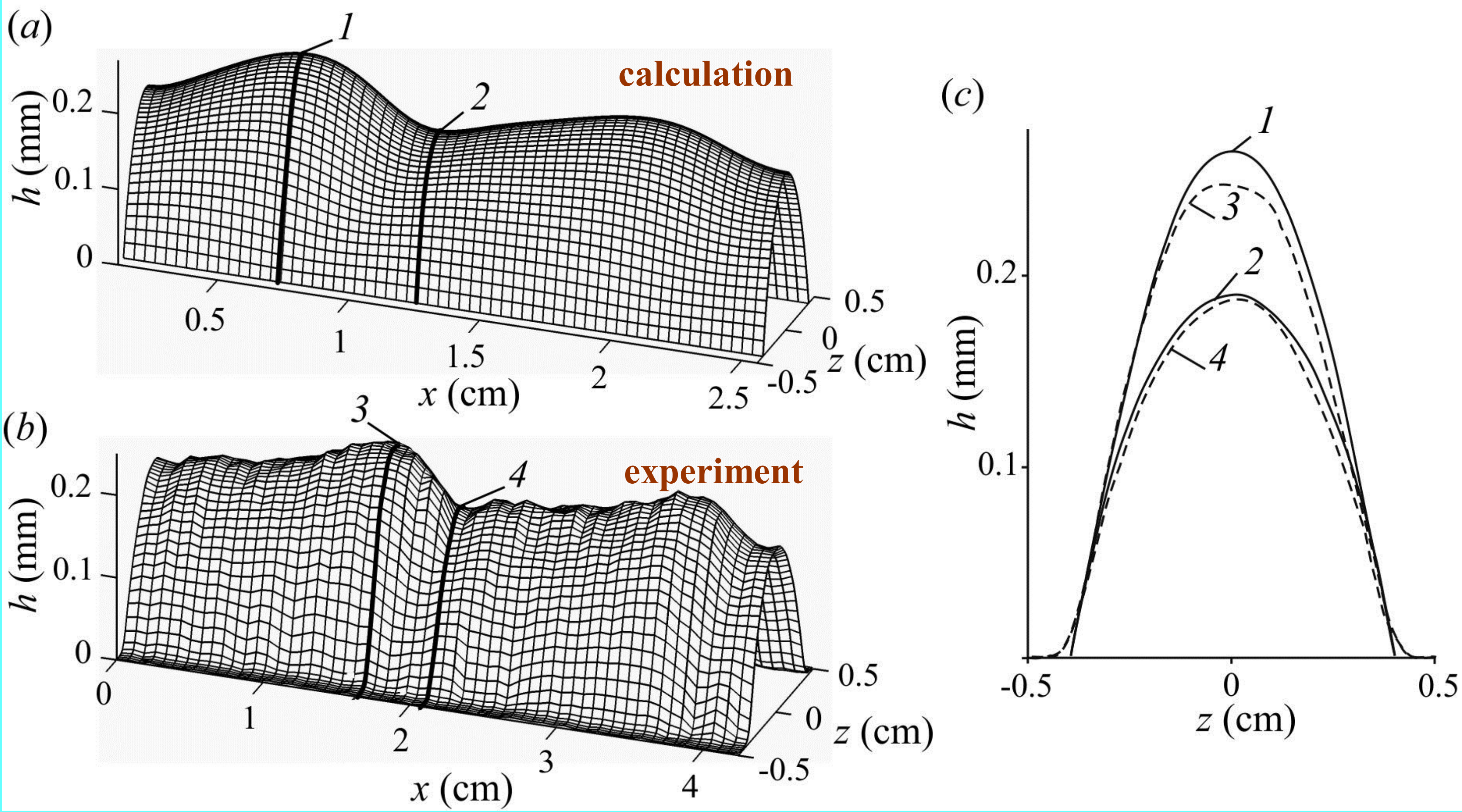

Shape of developed wave in WGS rivulet compared to the experimental data (Alekseenko *et al*. 2010) at $Re_m = 10$, $f = 15$ Hz.

(*a*) calculated 3D surface, (*b*) experimental 3D surface,

(*c*) cross-sections: (1, 2) calculation, (3, 4) experiment.

Wavy rivulet flow on vertical plate: theory

Velocity of developed nonlinear waves depending on amplitude at Re_m = 25

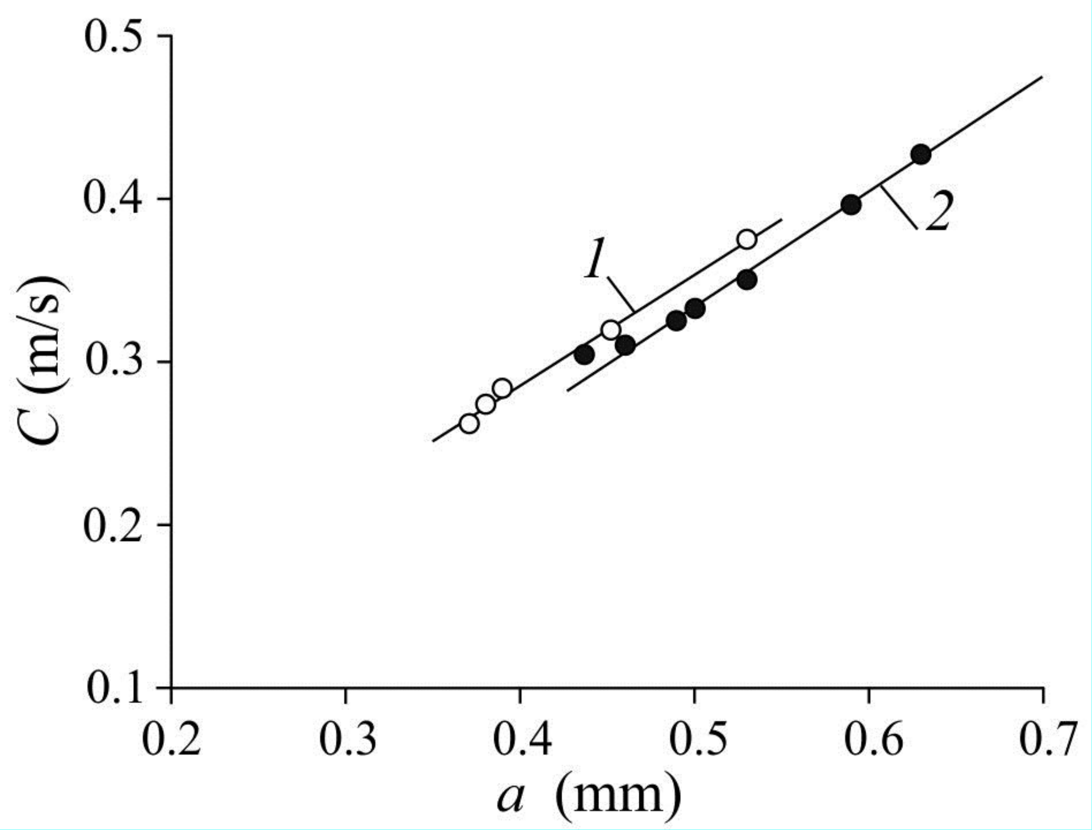

1 – WGS (frequency: 10, 15, 20, 25, and 30 Hz),
2 – WES (frequency: 5, 7, 10, 15, 17, 20, and 25 Hz).

Wavy rivulet flow on vertical plate: theory

Contact angle vs distance, f = 5 Hz, Re_m = 25

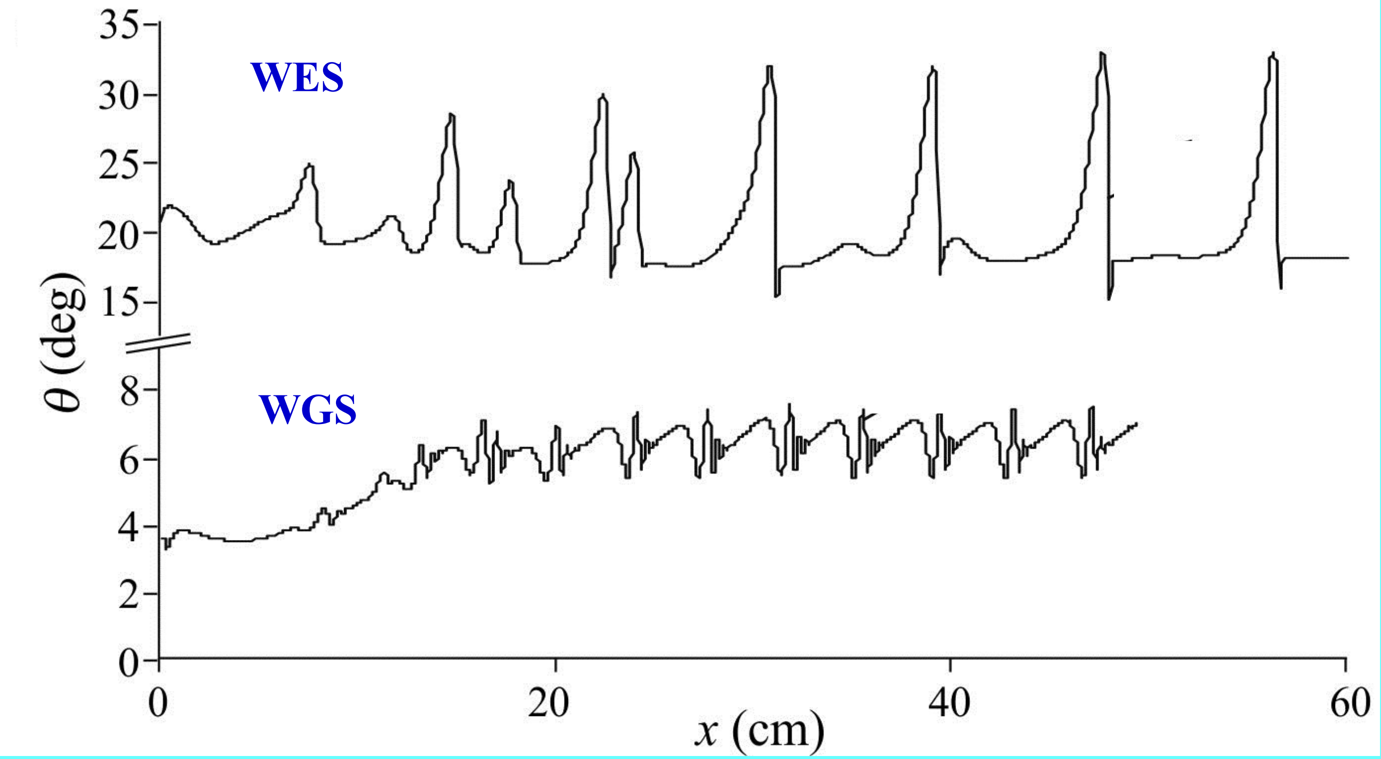

Alekseenko, Aktershev, Bobylev, Kharlamov, Markovich:
J. Fluid Mech., 2015 (in press)

Conclusion

3D regular linear and nonlinear waves in rectilinear rivulet flow along a vertical plate are first described on the basis of numerical simulation. The boundary condition of fixed contact line is accepted in theoretical model using experimental observations. It was demonstrated a good agreement between theory and experiment by 3D shape of rivulet waves.

4. INSTABILITIES IN ANNULAR TWO-PHASE FLOW

Wave structure of annular gas-liquid flow

Annular flow represents combined flow of liquid film on channel wall, high-velocity gas stream and liquid droplets entrained.

Gas stream

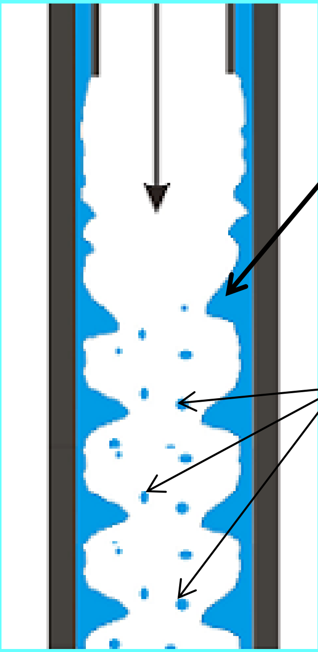

Liquid film

Droplets, entrained from film surface into the core of gas stream

For high gas velocities it could be said that transition to entrainment occurs at certain liquid flow rate irrespectively of gas velocity

One of entrainment mechanisms is disruption of ripples on disturbance waves' crests (observed by Woodmansee & Hanratty: 1969)

Flow map of transition to entrainment

Downward air-water annular flow, *d* = 15 mm

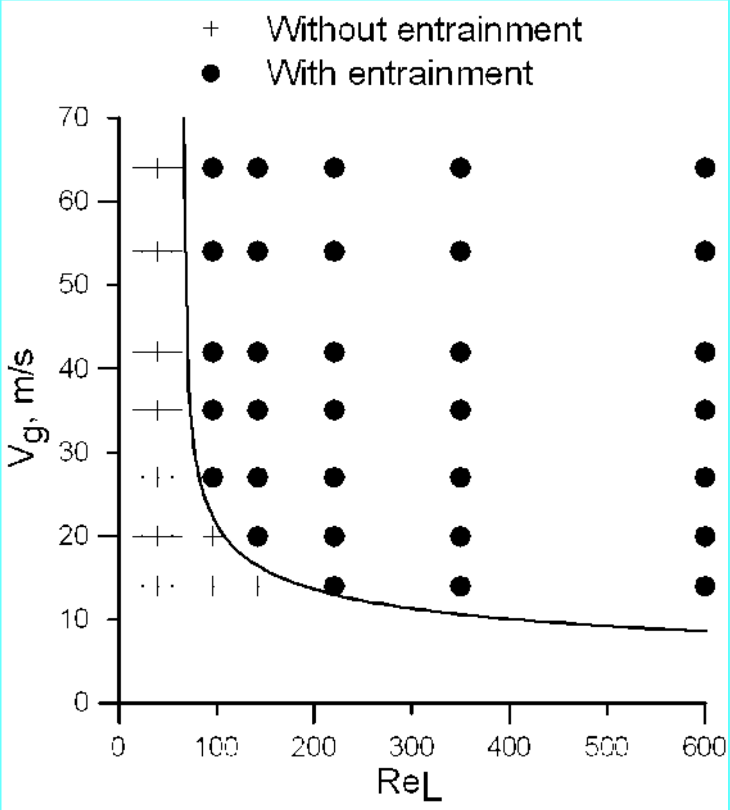

Wave structure of annular gas-liquid flow

Traditional description of wavy structure in annular flow

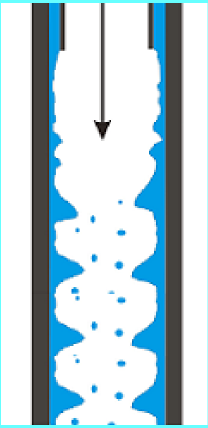

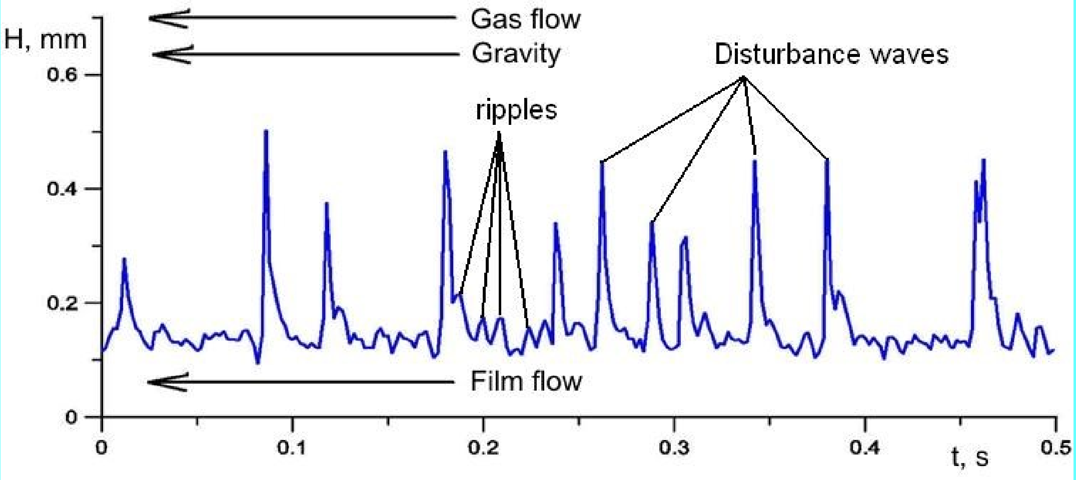

Flow with entrainment
$Re_L = 142$,
$V_g = 42$ m/s

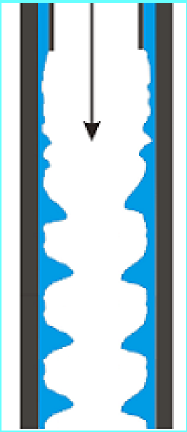

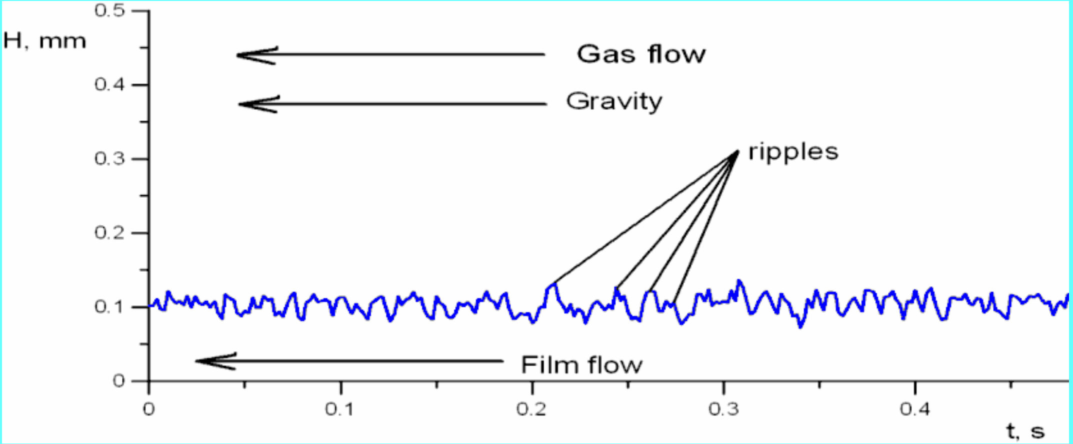

Flow without entrainment
$Re_L = 40$,
$V_g = 42$ m/s

1. Ripples are omnipresent at liquid film surface under intensive gas shear.
2. Transition to entrainment occurs due to inception of disturbance waves.

Wave structure of annular gas-liquid flow

Scheme of experimental setup for study of downward annular flow

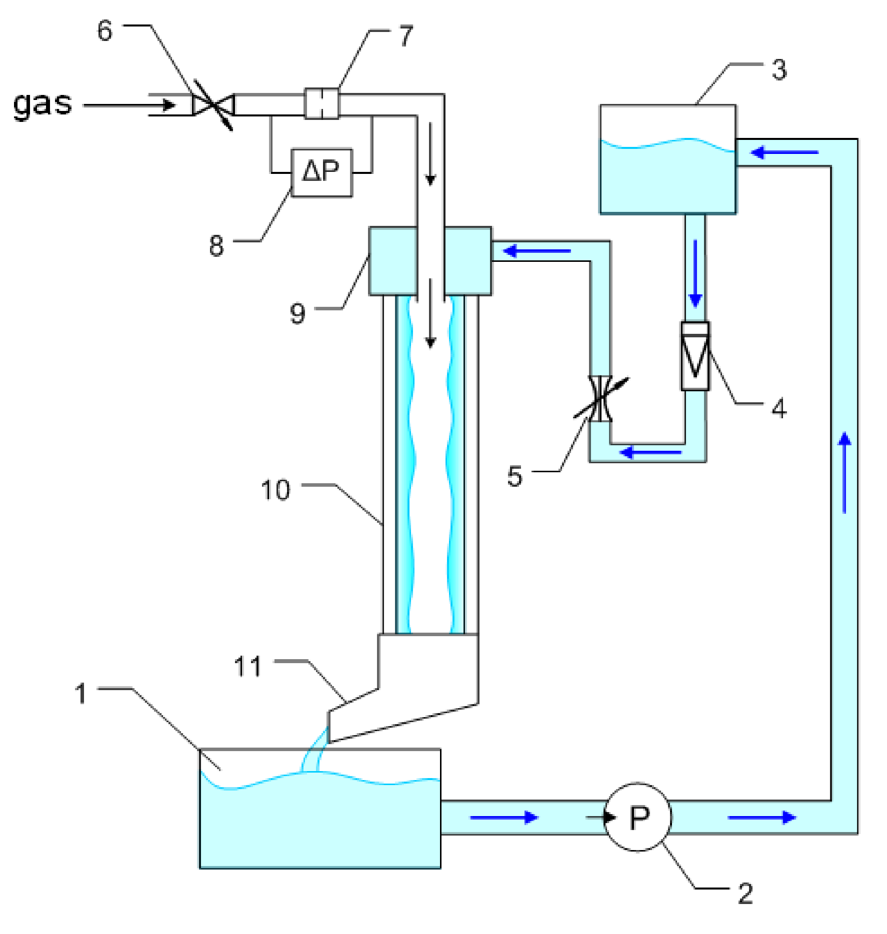

Flow parameters:
Tube's inner diameter d = 15 mm;
Liquid Reynolds numbers $Re_L = q/\pi d\nu$:
Re_L= 16 - 520;
Average gas velocities V_g = 18 - 80 m/s;
Distance from the inlet 5 - 60 cm;
Working liquids – water and water-glycerol solutions with ν = 1.5, 1.9, 3*10^{-6} m^2/s.

Inlet section

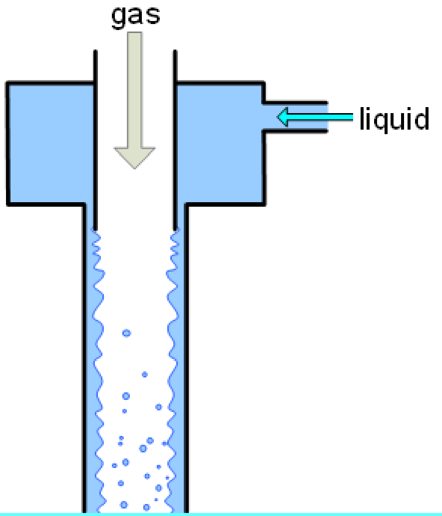

Storage tank (1); pump (2); pressure tank (3); liquid rotameter (4); valves (5-6); orifice meter (7); liquid manometer (8); gas-liquid distributor (9); working section (10); separator (11).

Wave structure of annular gas-liquid flow

High-speed modification of LIF technique: 2D-approach

Top view

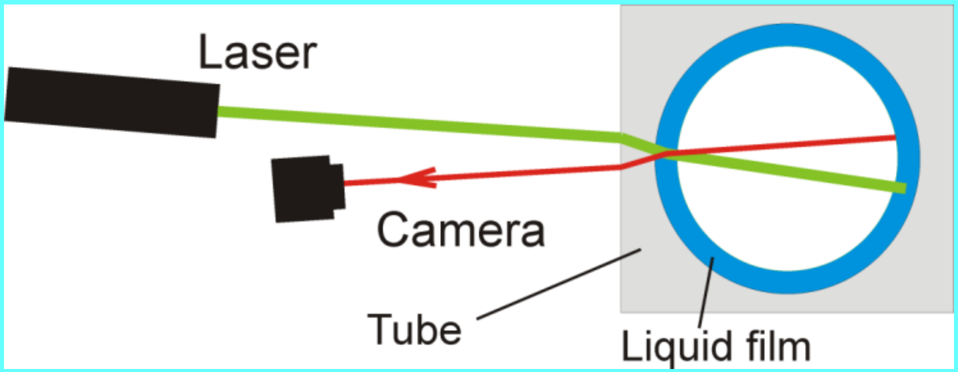

Side view

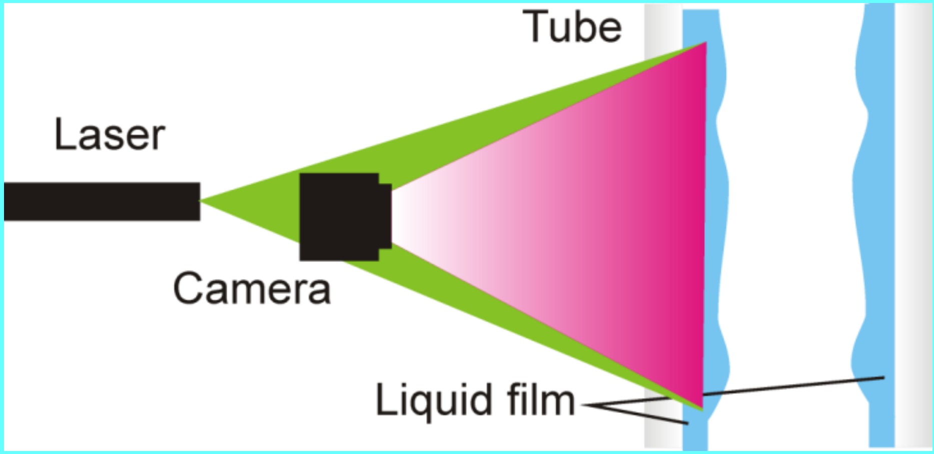

Light source: Continuous green laser, wavelength 532 nm, power 2 W

Fluorescent matter – Rhodamine 6G, in concentration 30 mg/l

Resolution (depends on task):

Camera sampling rate: 2 - 50 kHz;

Exposure time: 2 – 100 μs;

Spatial resolution: 0.1 mm;

Accuracy: 2 – 3%

Alekseenko, Antipin, Cherdantsev, Kharlamov, Markovich: Microgravity Science and Technology, 2008

Wave structure of annular gas-liquid flow

No-entrainment regimes. Primary and secondary waves

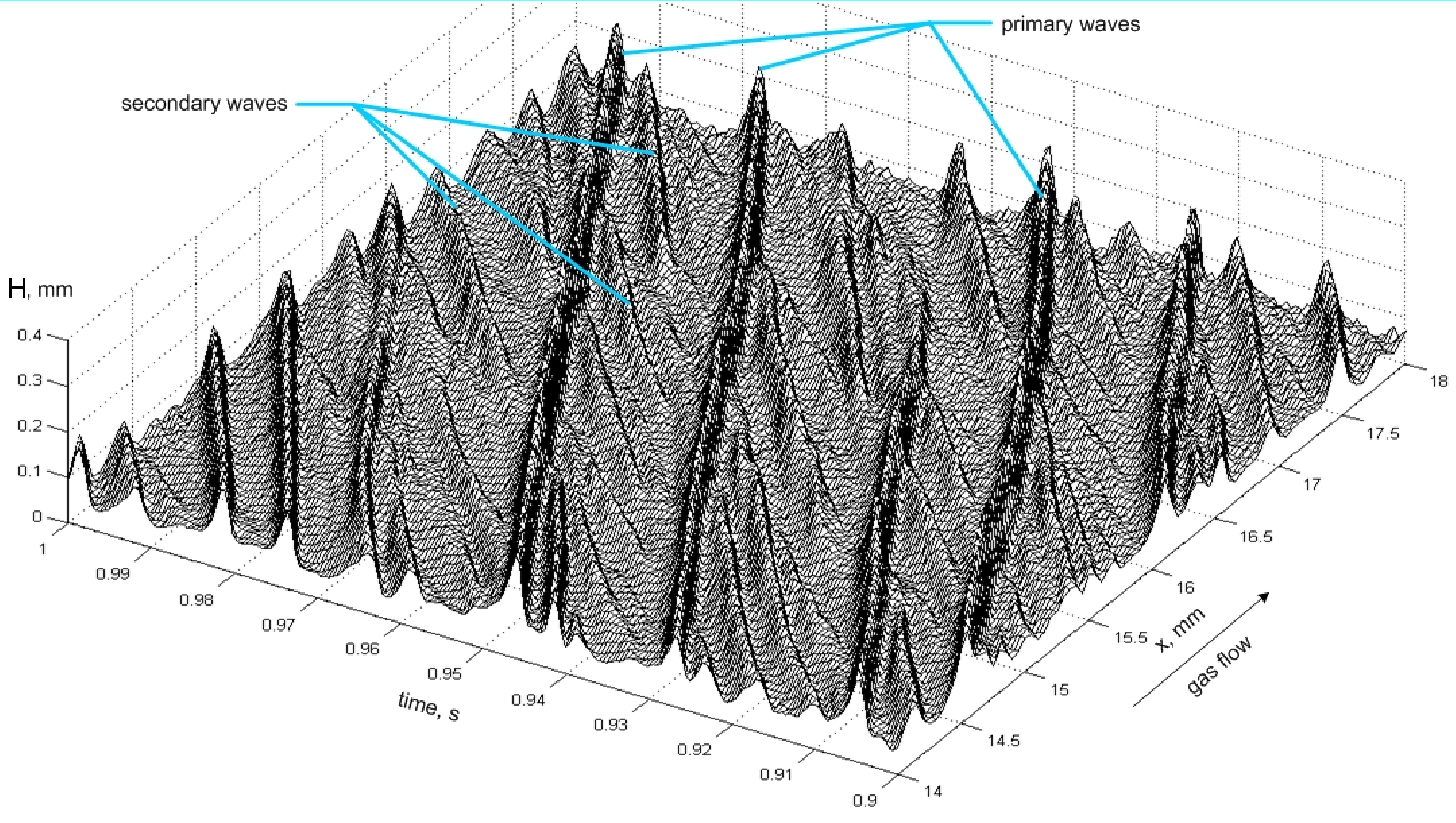

Primary and secondary waves in regimes without entrainment.
All secondary waves are generated at the back slopes of primary waves.

***Re_L* = 40, *V_g* = 27 m/s.**

Wave structure of annular gas-liquid flow

No-entrainment regimes. Re_L = 40.

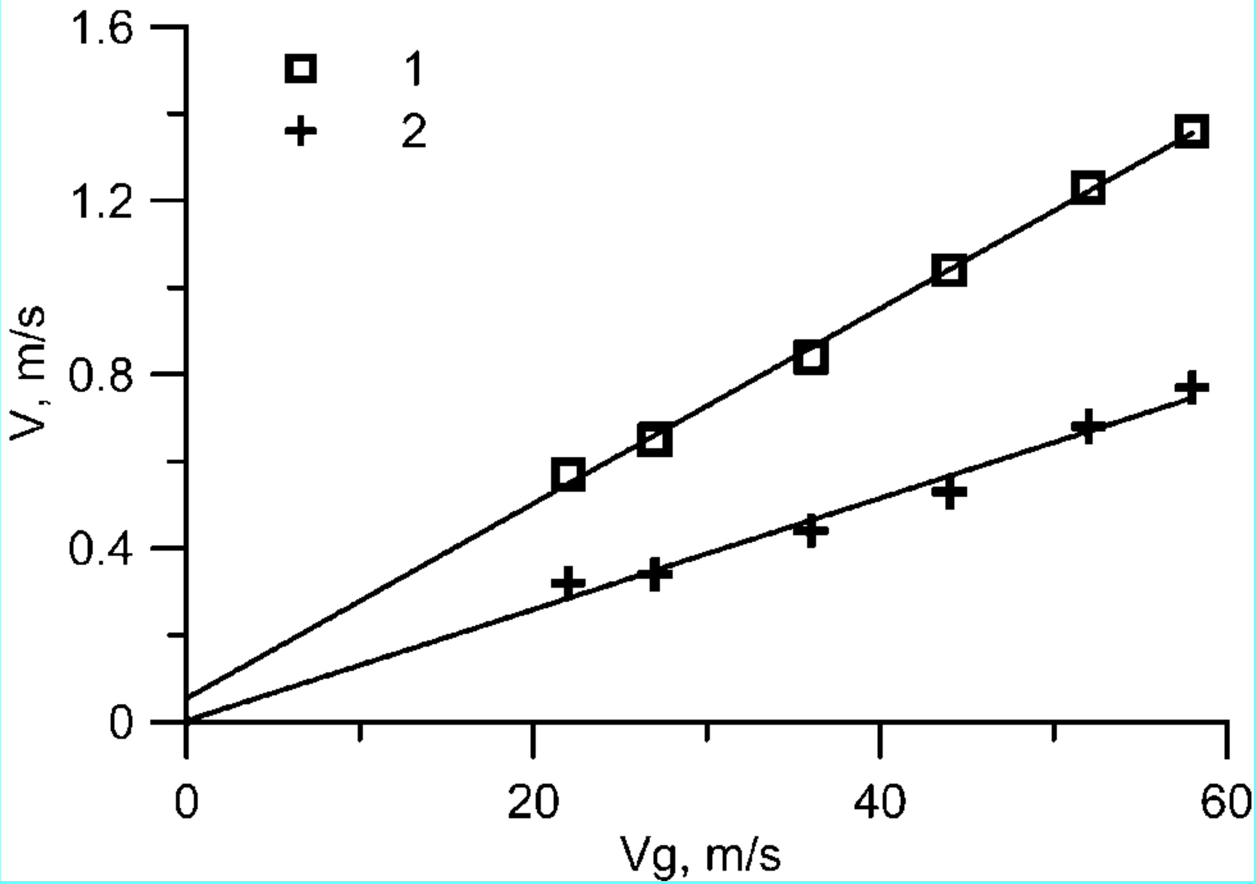

1 - primary waves

2 - secondary waves

Alekseenko, Cherdantsev, Cherdantsev, Markovich:
Microgravity Science and Technology, 2009

Wave structure of annular gas-liquid flow

Entrainment regimes. Disturbance waves and two types of ripples: fast and slow ripples

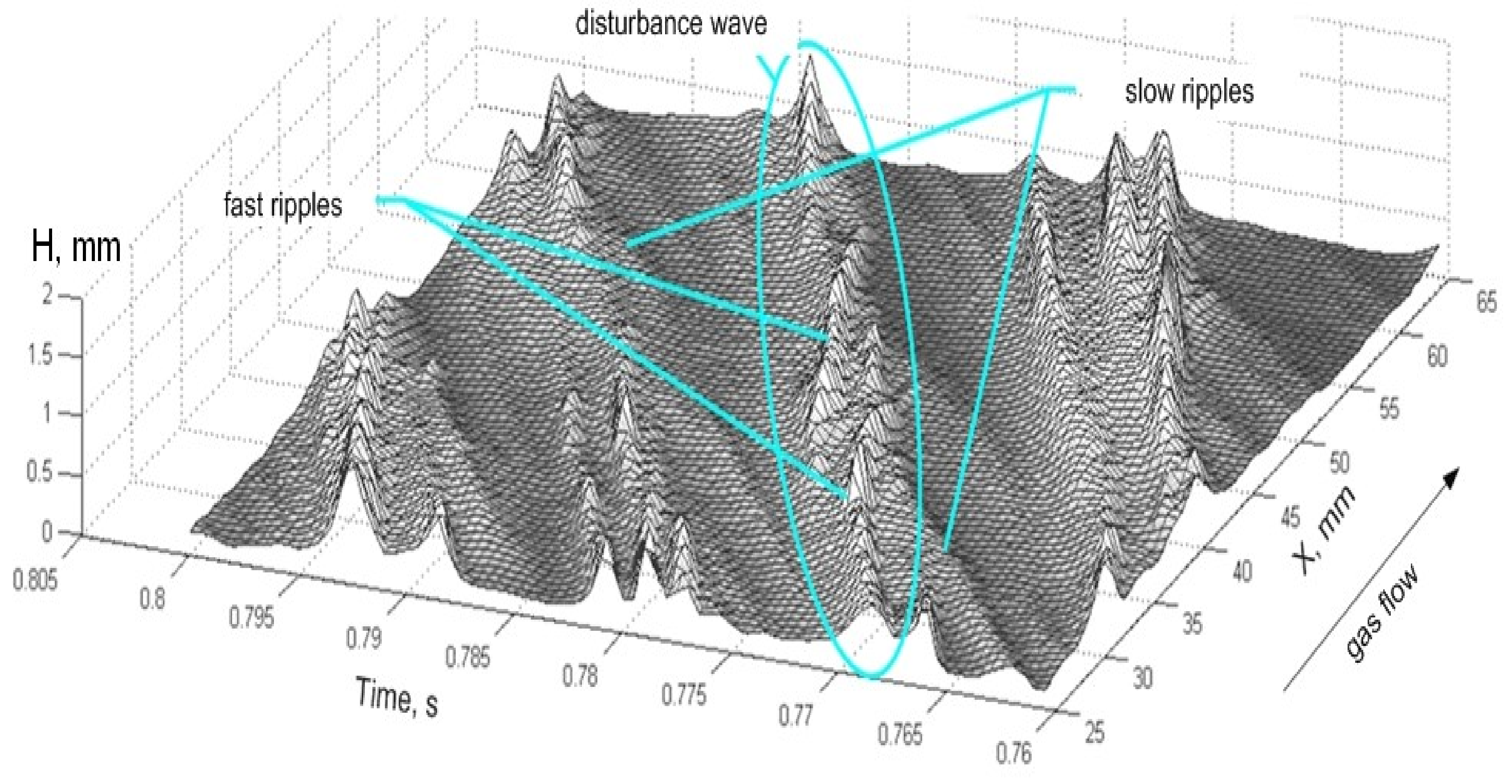

Fast ripples on the disturbance wave and slow ripples on the residual layer. $Re_L = 350$, $V_g = 27$ m/s.

Wave structure of annular gas-liquid flow

Entrainment regimes. $Re_L = 350$

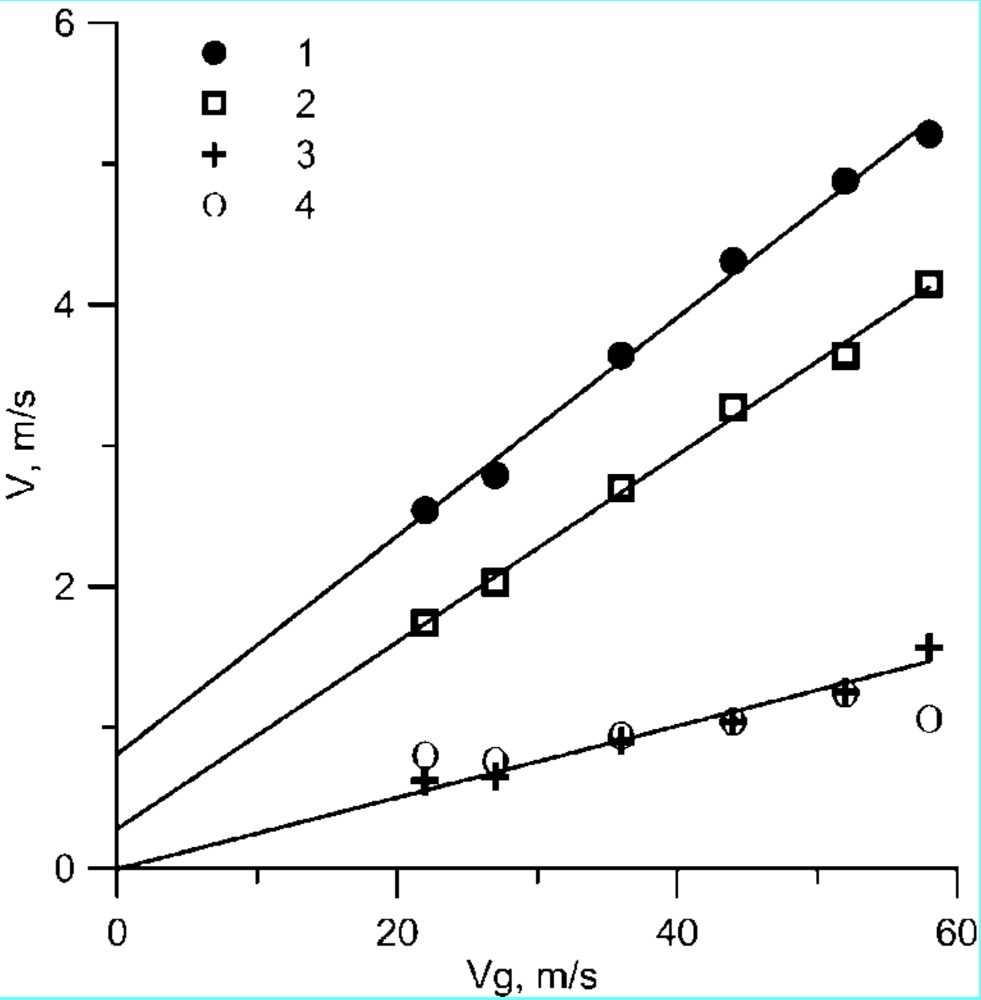

1 - fast ripples

2 - disturbance waves

3 - slow ripples

Alekseenko, Cherdantsev, Cherdantsev, Markovich:
Microgravity Science and Technology, 2009

Wave structure of annular gas-liquid flow

Possible explanation of the formation of fast and slow ripples

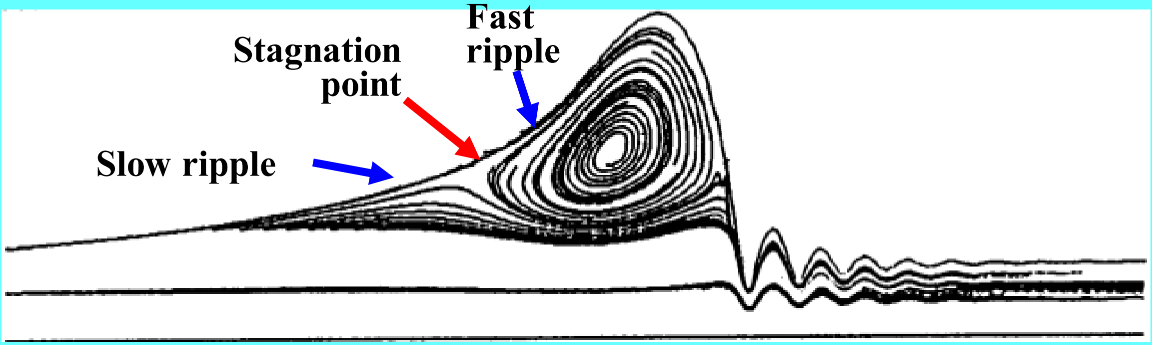

Stream lines in the reference system of the wave (Miyara, 1999)

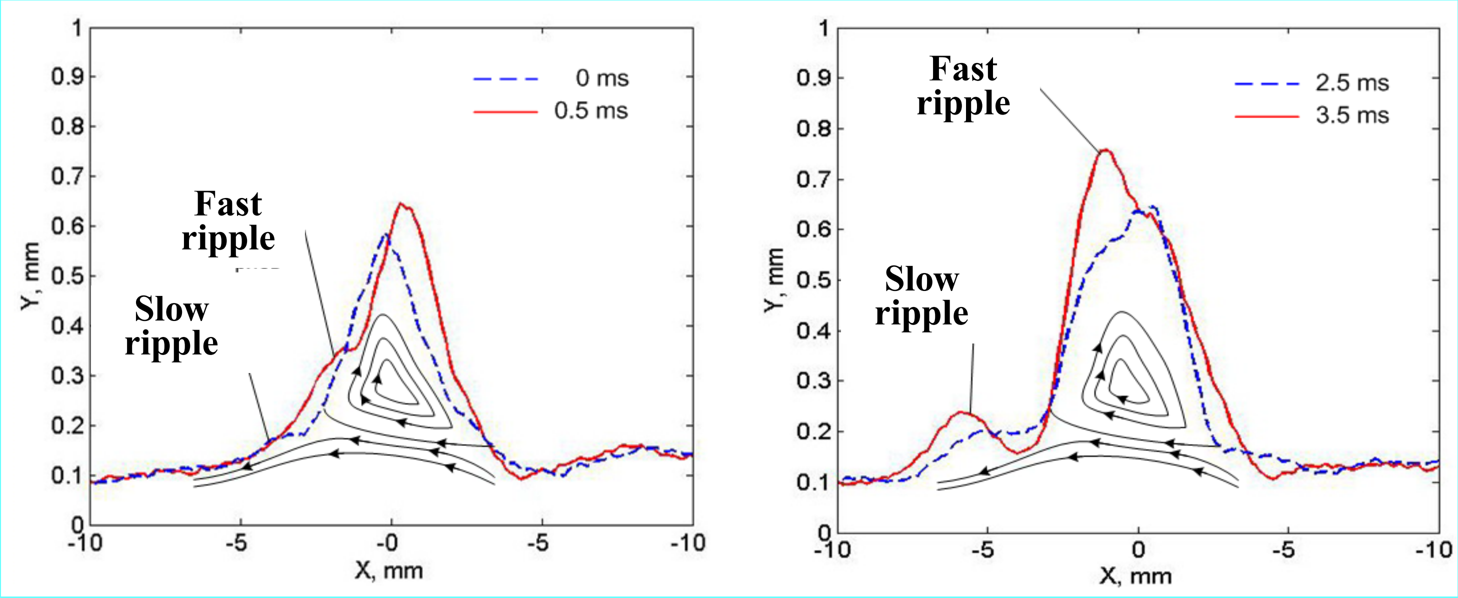

Evolution of the wave profile

Alekseenko, Antipin, Cherdantsev, Kharlamov, Markovich: Physics of Fluids, 2009

Wave structure of annular gas-liquid flow

Droplet images in LIF-data

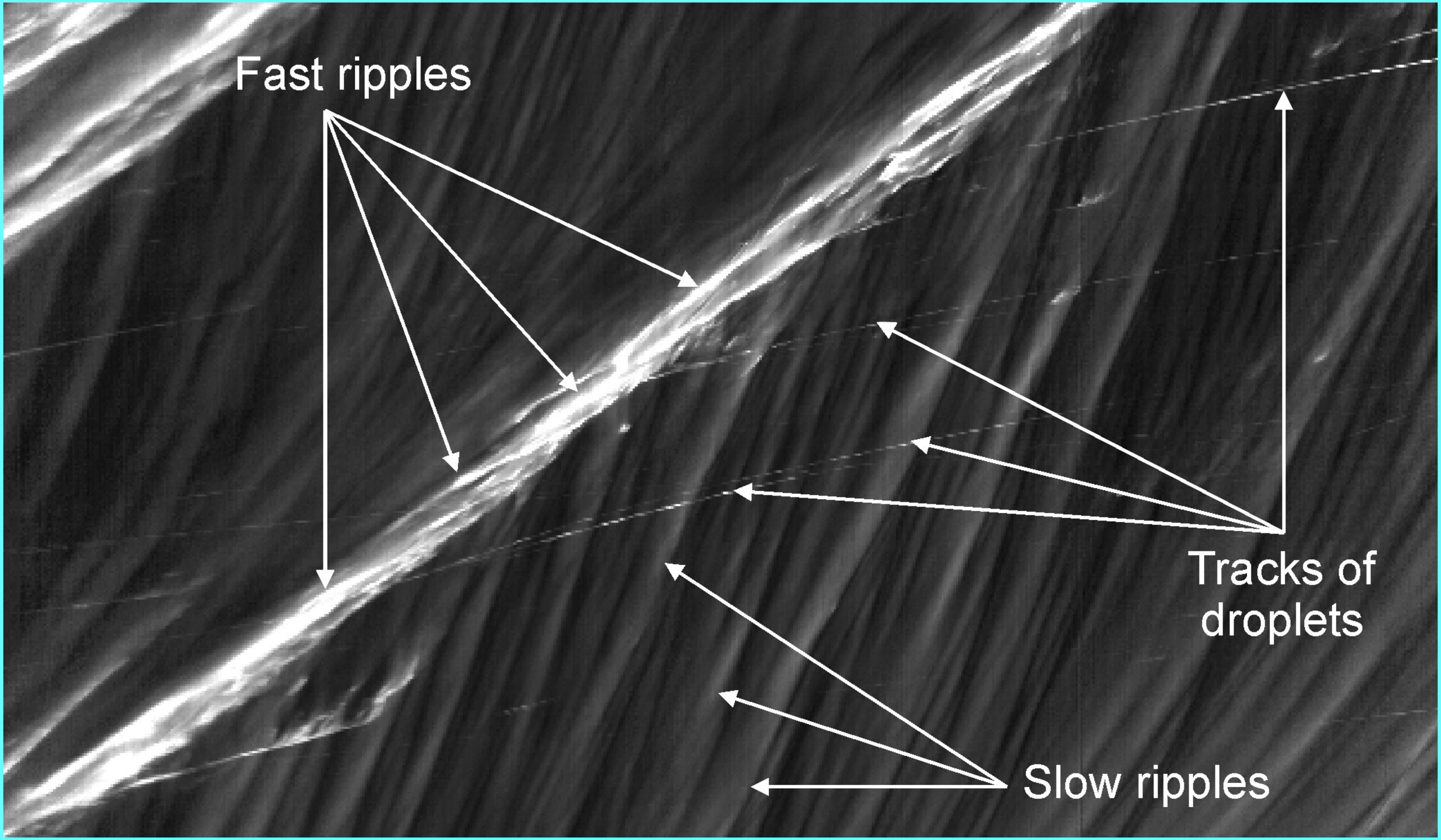

Size of the image is 12 cm * 35 ms. Re_L **= 220,** V_g **= 27 m/s, water.**

Wave structure of annular gas-liquid flow

Velocity of droplets after entrainment

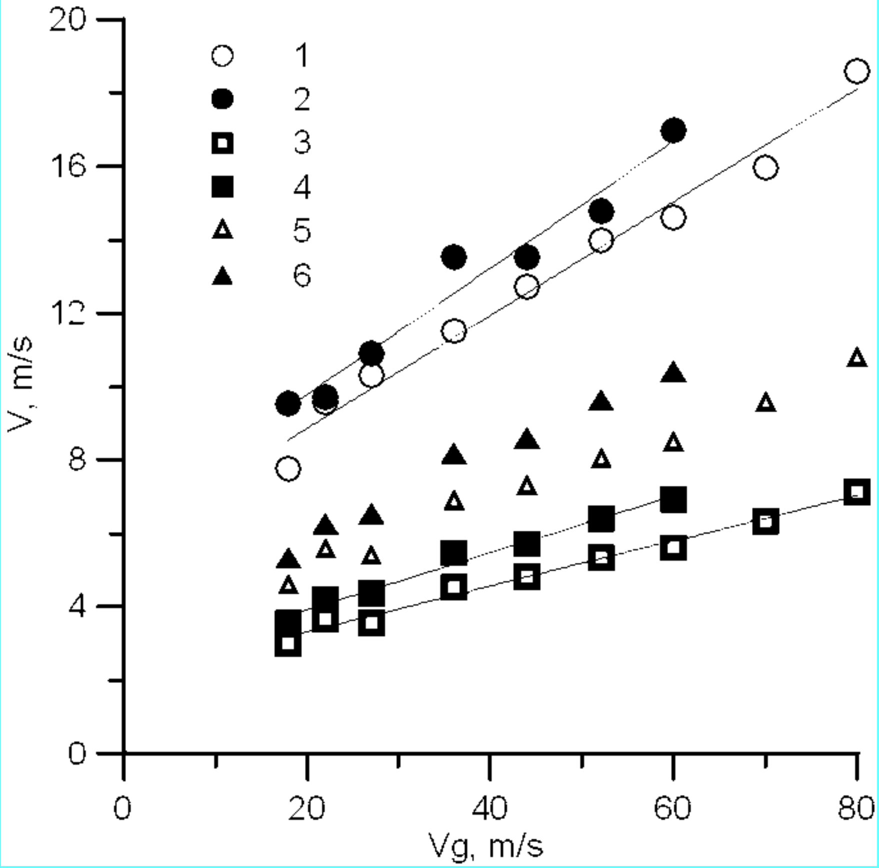

1 – droplets, $Re_L = 180$

2 – droplets, $Re_L = 500$

5 – fast ripples, $Re_L = 180$

6 – fast ripples, $Re_L = 500$

3 – disturbance waves, $Re_L = 180$

4 – disturbance waves, $Re_L = 500$

The new-created droplets move with initial velocity about 1.5 times higher than that of fast ripples. Velocity difference between 1-2 and 5-6 denotes large momentum gained by droplets in process of fast ripples‘ rupture.

Alekseenko, Cherdantsev, Markovich, Rabusov: Atomization & Sprays, 2014

Wave structure of annular gas-liquid flow

High-speed modification of LIF technique - 3D-approach

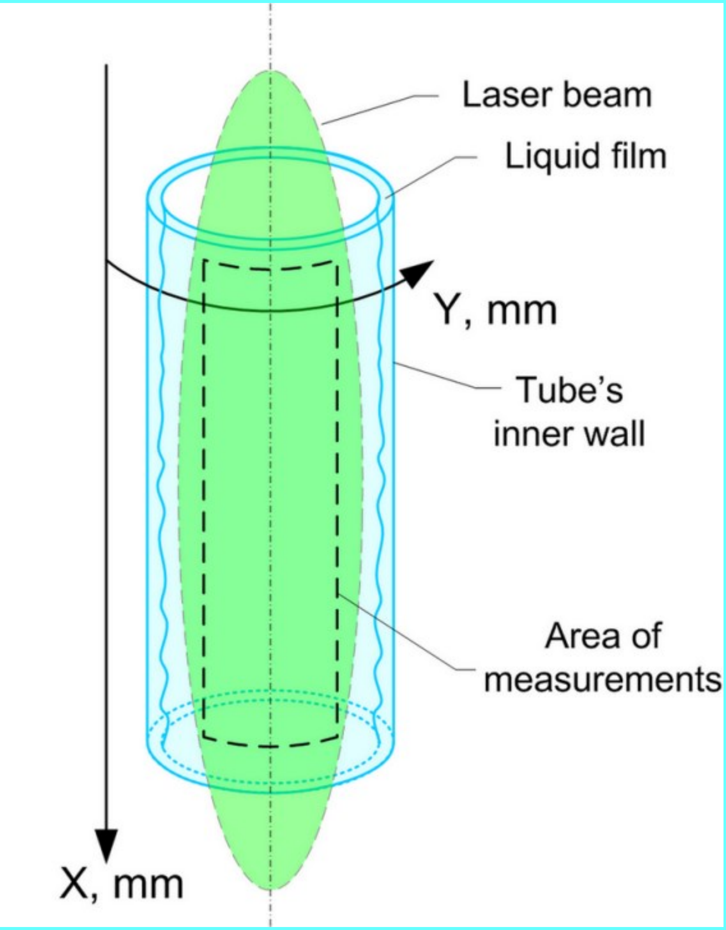

High-speed camera PCO.1200 with rectangular matrix is used;

For 3D-experiments, laser light is spread on much larger area, and local illumination decreases greatly.

Temporal resolution is limited by local illumination.

Measures to increase temporal resolution:
1. Laser with much higher (2 W) power was used for excitation of fluorescent light;
2. Water-glycerol solution with viscosity of 3 cSt was used as working liquid, since
a) film thickness is thicker for the same liquid Reynolds numbers
b) brightness of fluorescent light is higher in WGS than in water, other things being equal.

Camera was focused on the nearest wall of the tube to minimize registration of light emitted by the film flowing on the distant wall of the channel.
500 Hz temporal resolution was reached.

Alekseenko, Cherdantsev, Cherdantsev, Isaenkov, Kharlamov, Markovich: Exp. Fluids, 2012

Wave structure of annular gas-liquid flow

3D-approach: wavy structure of liquid film in regimes without entrainment

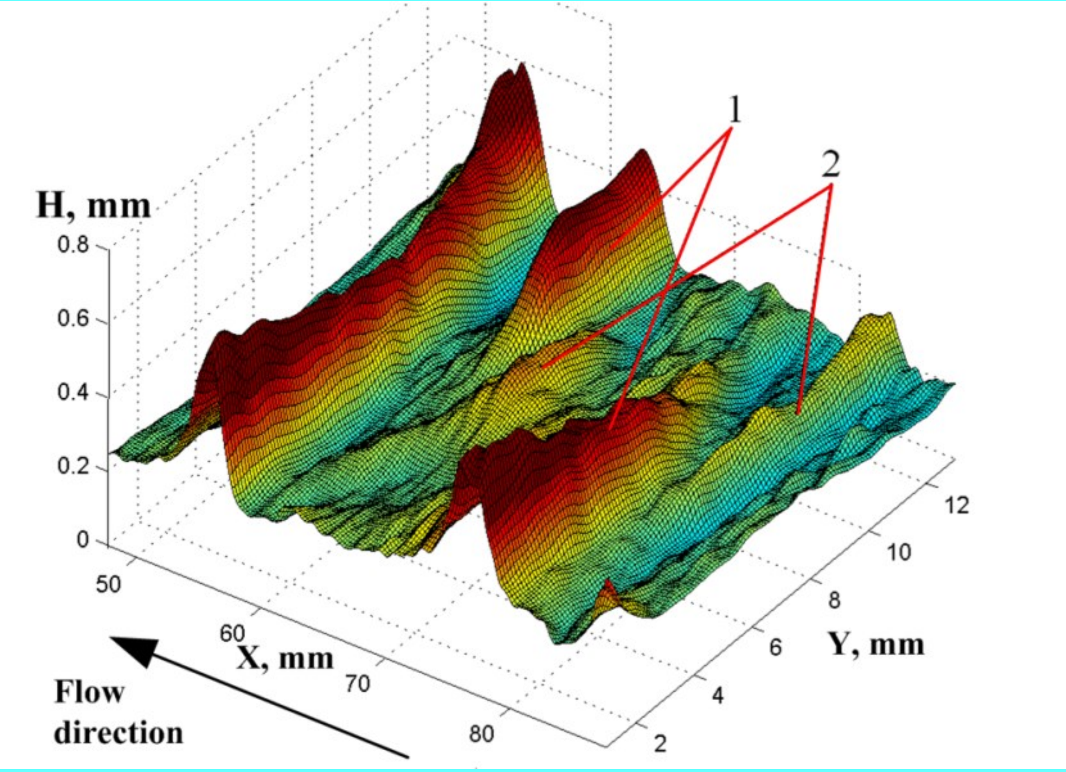

Appearance of edges of primary waves means that not all the primary waves form full rings around the circumference of the pipe.

The edges of primary waves do also generate secondary waves, as well as central parts of primary waves.

1 – Edges of primary waves. 2 – Secondary waves, generated at the edges of primary waves.
Re_L = 18, WGS, V_g =18 m/s.

Conclusion

Interfacial waves in annular two-phase flow are studied in detail with using high-speed modification of LIF technique. It was demonstrated the existence of two-wave structure of interphase. In case of flow with droplet entrainment small ripples consist of fast and slow ones. Namely fast ripple is responsible for droplet entrainment from the crests of large disturbance waves. The examples of measuring 3D shape of interface are presented.

5. TRANSPORT PHENOMENA:

Wave effect on condensation and evaporation

Wave effect on condensation

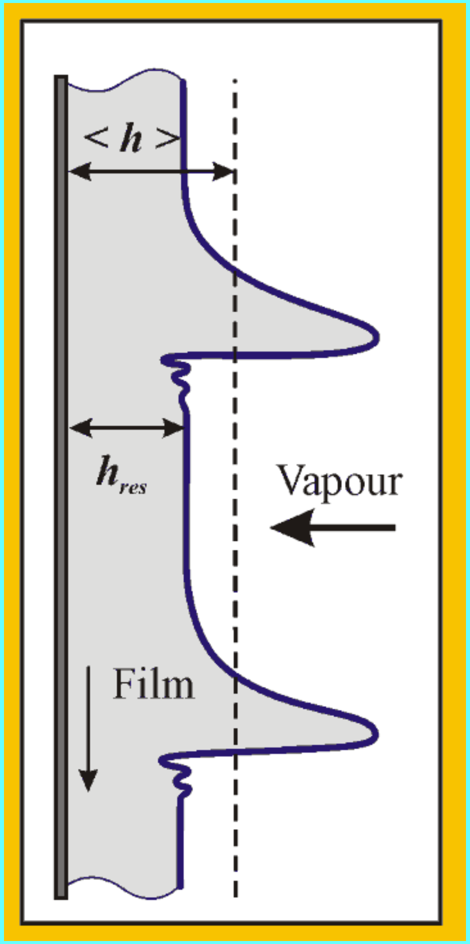

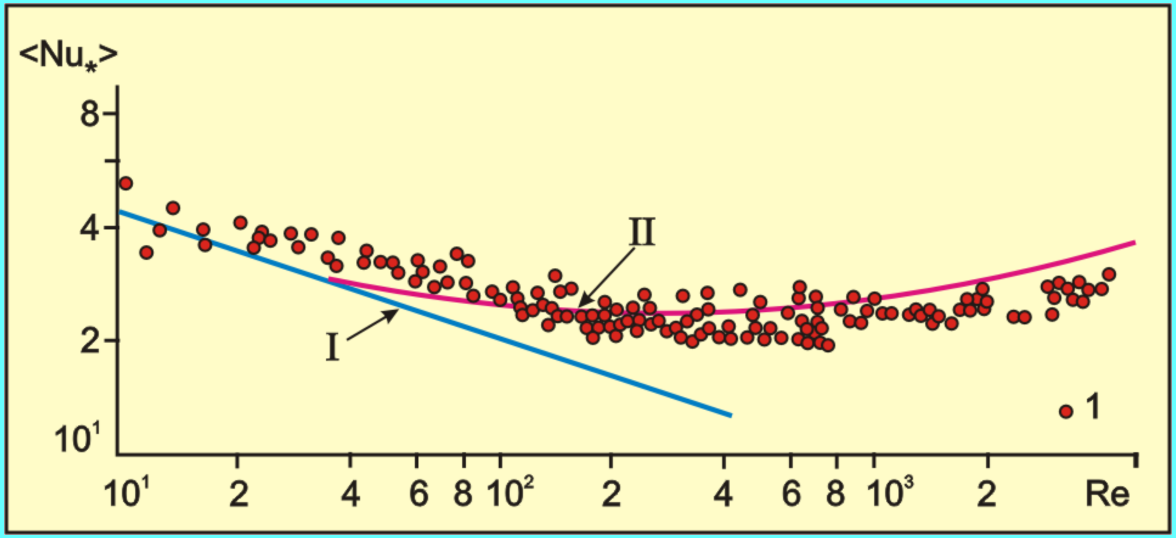

1 – experiment (Gogonin et al, 1980)

I – Nusselt theory

II – calculation on the basis of (1)

$$a \approx l \,/ h_{res} \qquad (1)$$

Statement of the problem

Film with condensation

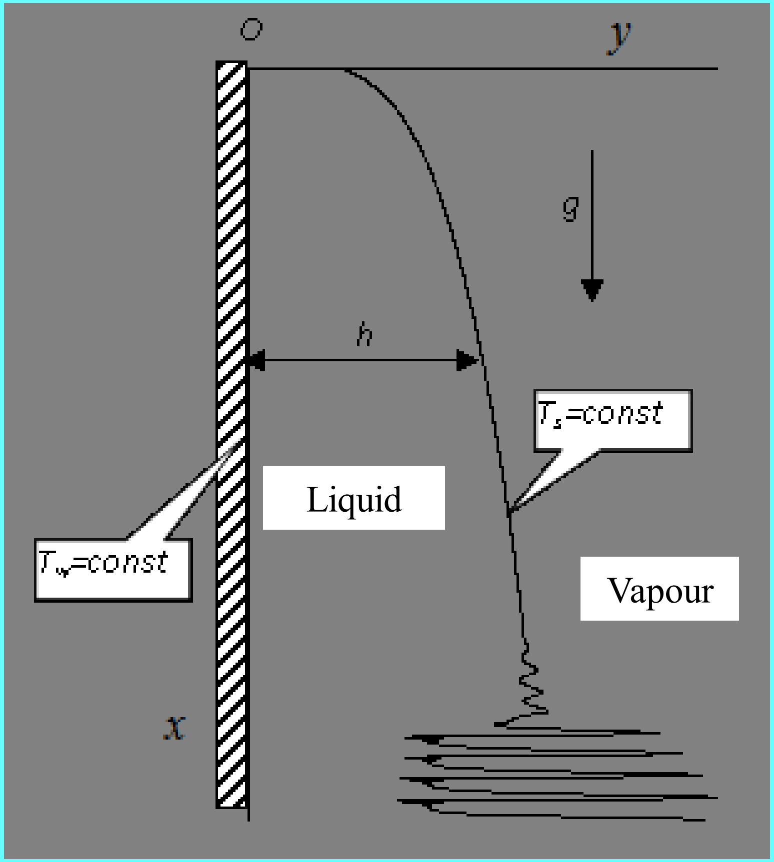

Film with evaporation

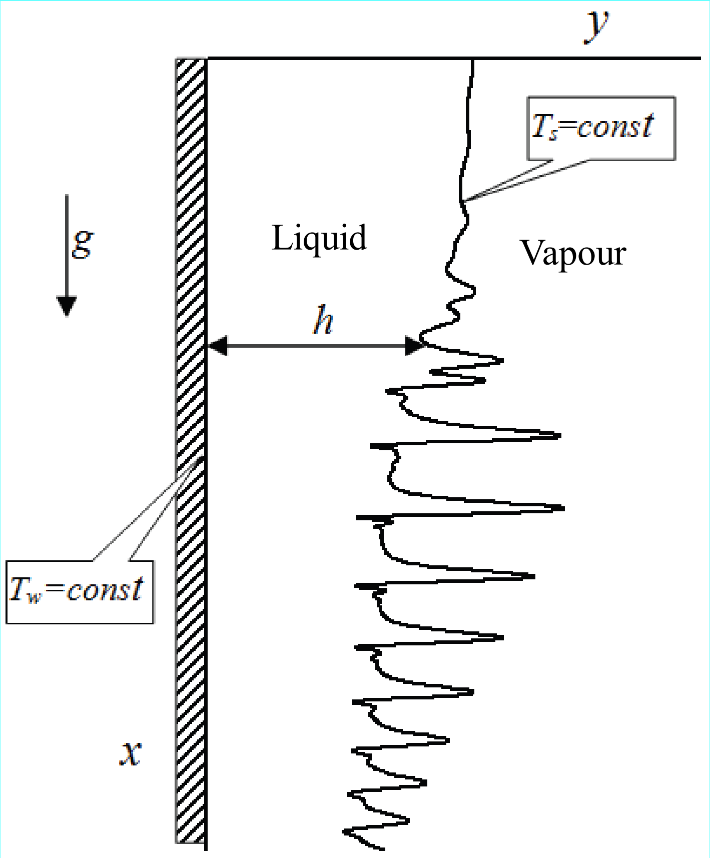

1) **Wall temperature $T_w = const$; saturated vapor with the temperature $T_s = const$.**
2) **A liquid film is a main contributor to the thermal resistance.**
3) **The contribution of the reactive force due to phase transition is neglected.**
4) **Film surface perturbation is considered to be the long-wave**
5) **Thermophysical properties are considered constant.**

Dimensionless equations of non-isothermal film flow

$$\frac{\partial q}{\partial t}+\frac{\partial}{\partial x}\left(\frac{6\boxed{F_0}q^2}{5h}\right)=\frac{3}{\chi\, Re_m}\left(h-\boxed{\frac{F_1 q}{h^2}}\right)+\chi^2 We h\frac{\partial^3 h}{\partial x^3},$$

$$\frac{\partial h}{\partial t}+\frac{\partial q}{\partial x}=\boxed{\pm\frac{A}{\chi\, Re_m\, h}},$$

$$\frac{\partial \theta}{\partial t}+u\frac{\partial \theta}{\partial x}+\frac{W}{h}\frac{\partial \theta}{\partial \eta}=\frac{1}{\chi\, Re_m\, Pr\, h^2}\frac{\partial^2 \theta}{\partial \eta^2}.$$

Here q is flow rate,
h is film thickness,
θ is liquid temperature,

$$F_0=1-A/(4+A)^2,$$
$$F_1=1+A/(4+A)$$
$$A=\varepsilon\frac{\partial\theta}{\partial\eta}\Big|_{\eta=1}$$

Dimensionless criteria:

$Re_m=gh_m^3/3\nu^2$ **– Reynolds number at the inlet**

$\boxed{\varepsilon=c_p\Delta T/(r\cdot Pr)}$ **– phase transition intensity**

$Fi=\sigma^3/\rho^3 g\nu^4$ **– Kapitsa number,** **Pr – Prandtl number**

$\chi=h_m/l$ **– linear scales ratio**

$We=\left(3Fi/Re_m^5\right)^{1/3}$ **– Weber number**

$Nu(x,t)=\dfrac{1}{(3\mathrm{Re}_m)^{1/3}h(x,t)}\dfrac{\partial\theta}{\partial\eta}\Big|_{\eta=0}$ **– Nusselt number**

Aktershev, Alekseenko: Phys. Fluids, 2013

Natural and forced waves

Natural waves appear due to flow instability.

Forced waves are generated by small flow rate pulsations at the inlet.

The equations were solved by finite-difference method with an implicit iteration scheme. The energy equation was solved by the sweep method with boundary conditions on the wall and on the film surface: $\theta\big|_{\eta=1} = 1,\ \theta\big|_{\eta=0} = 0.$

Boundary conditions at the inlet:

$$q(0,t) = q_0\left(1 + Q_a \sin 2\pi f t\right),\quad h(0,t) = 1,\qquad \theta(0,\eta,t) = \eta$$

Here q_0 – undisturbed flow rate, Q_a – small amplitude,
f – given flow rate pulsation frequency.

Initial conditions:

$$\theta(x,\eta,0) = \eta,\quad h(x,0) = \left(1 \pm \frac{4\varepsilon\left(F_1 + 2F_0\varepsilon/3\right)x}{3\chi\,\mathrm{Re}_m}\right)^{1/4},\quad q(x,0) = \frac{h^3}{F_1 + 2F_0\varepsilon/3}$$

All calculations were carried out for water at t = 373 K (Pr = 1.75, $Fi^{1/3}$ = 14 700)

Evolution of natural waves

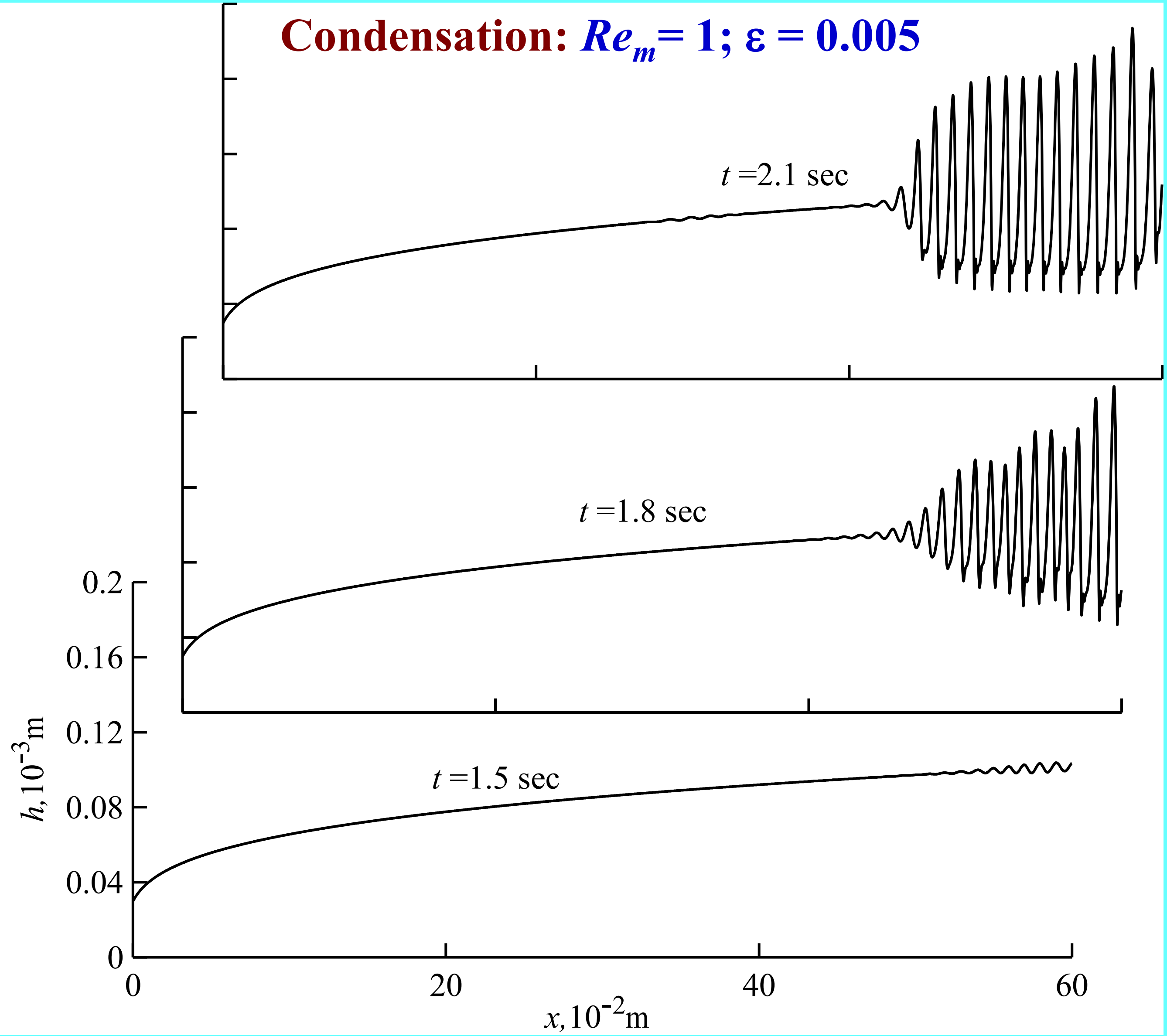

Emergence of natural waves at a section where $Re > Re_{cr}$

Forced waves

Condensation: $Re_m = 1$; $\varepsilon = 0.005$

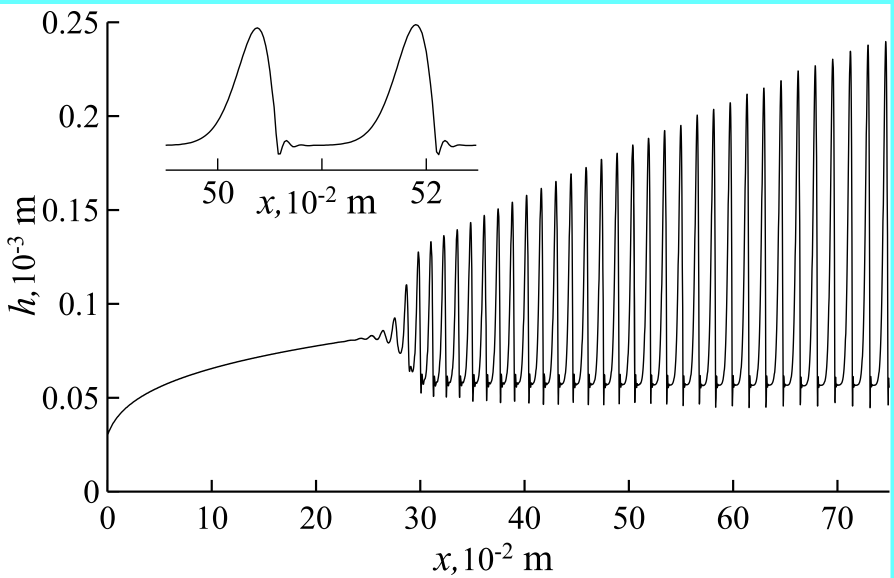

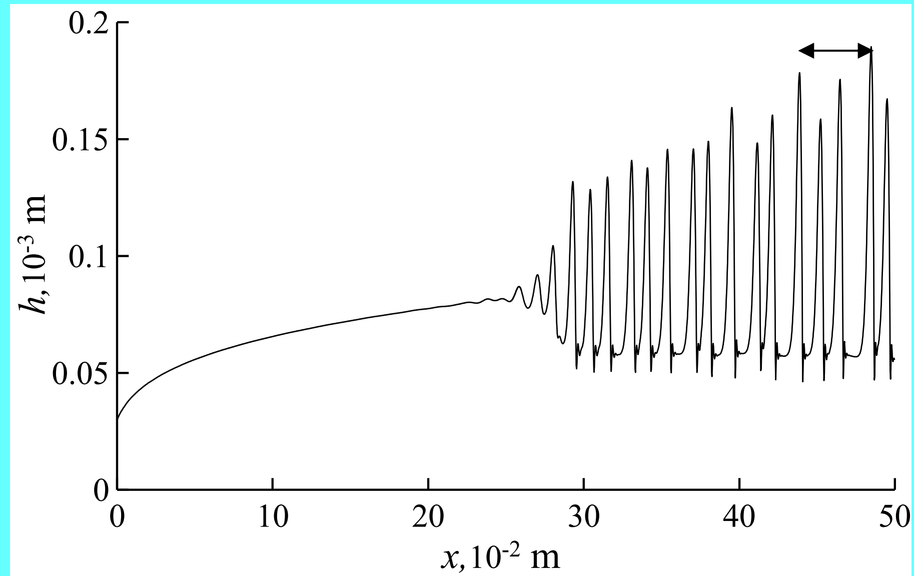

Waves with a frequency 18 Hz. Wave structure is shown in detail in the left upper part.

Amplitude of developed waves increases with distance from the inlet.

Waves with a frequency of 6 Hz. Double-arrow section corresponds to «wave length».

Intermediate peaks appear at low frequencies.

Wave effect on condensation

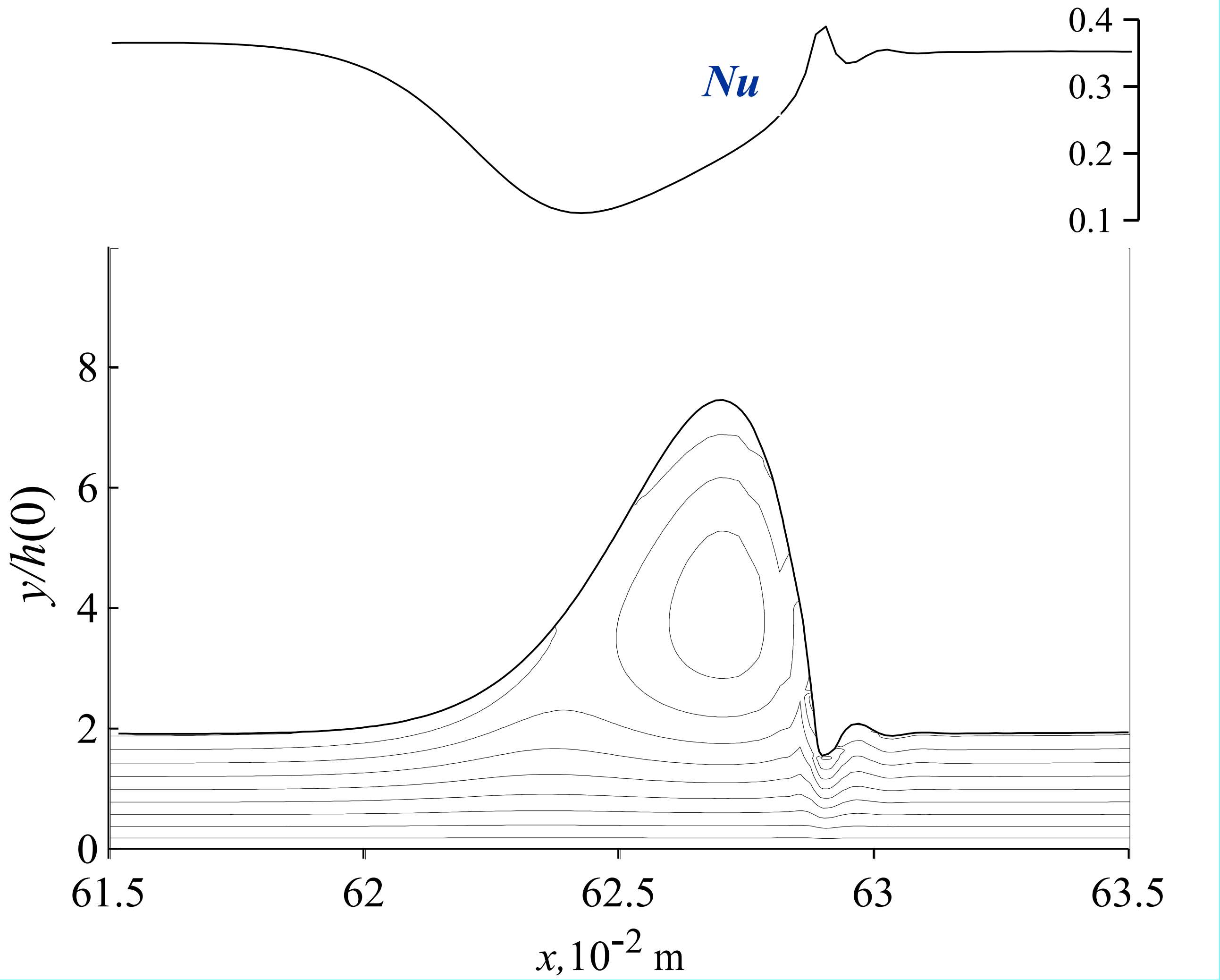

Spatial distribution of Nusselt number along the wave

The streamlines in a reference frame moving with the wave.

Wave velocity 0.27 m/s. Recirculation zone is observed near the wave crest.

The main contribution to the heat transfer enhancement due to waves is caused by area between the peaks, because film thickness is minimal there; while the length of this area is substantially greater than the length of the peak.

Wave effect on condensation

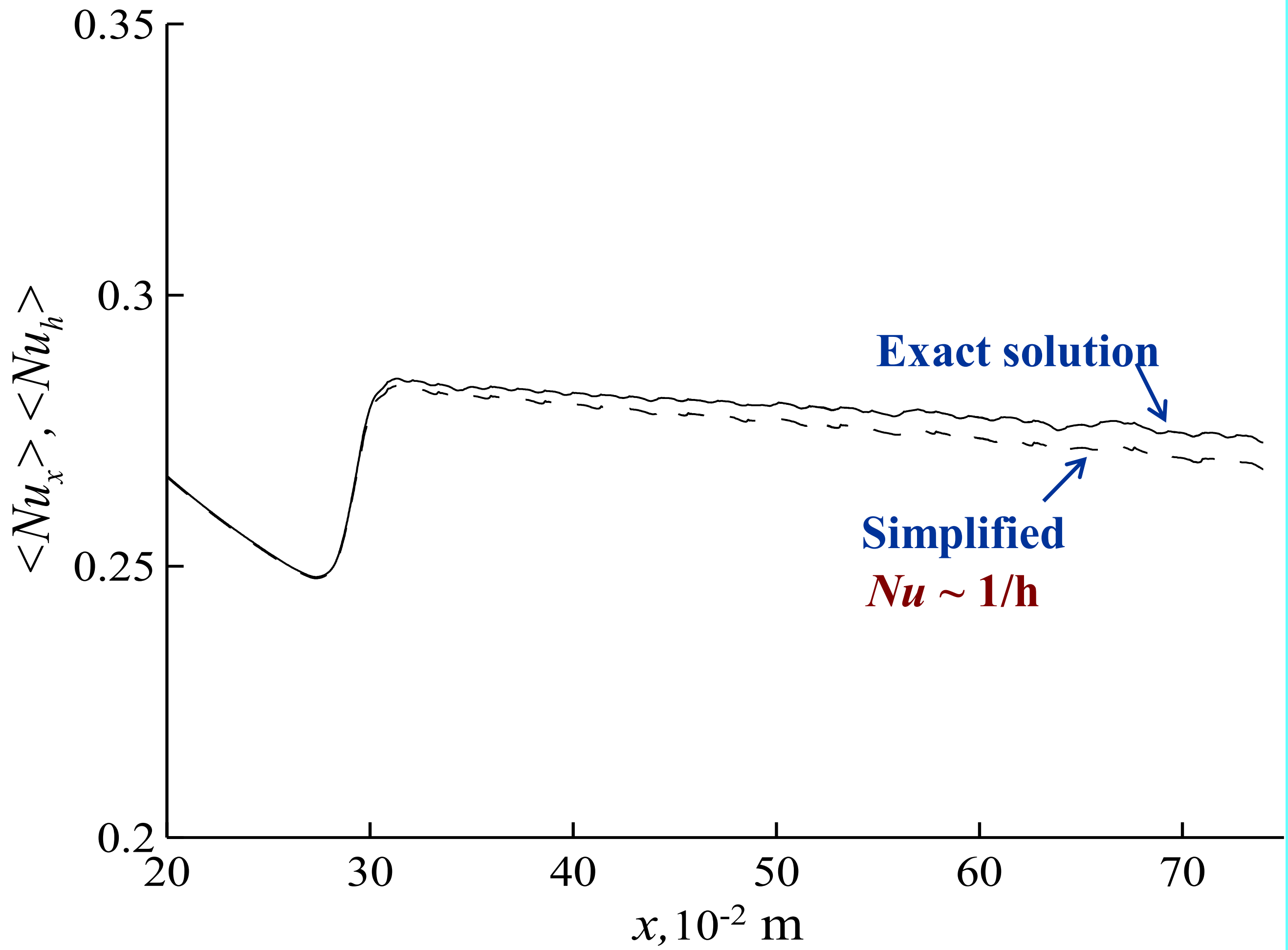

Dependence of time-averaged Nusselt number on coordinate at $f = 18$ Hz; solid line is exact solution; dashed line corresponds to calculation by simplified formula:

$$\langle Nu_h \rangle = \left(3\,\mathrm{Re}_m\right)^{-1/3} \langle 1/h \rangle$$

Wave effect on condensation

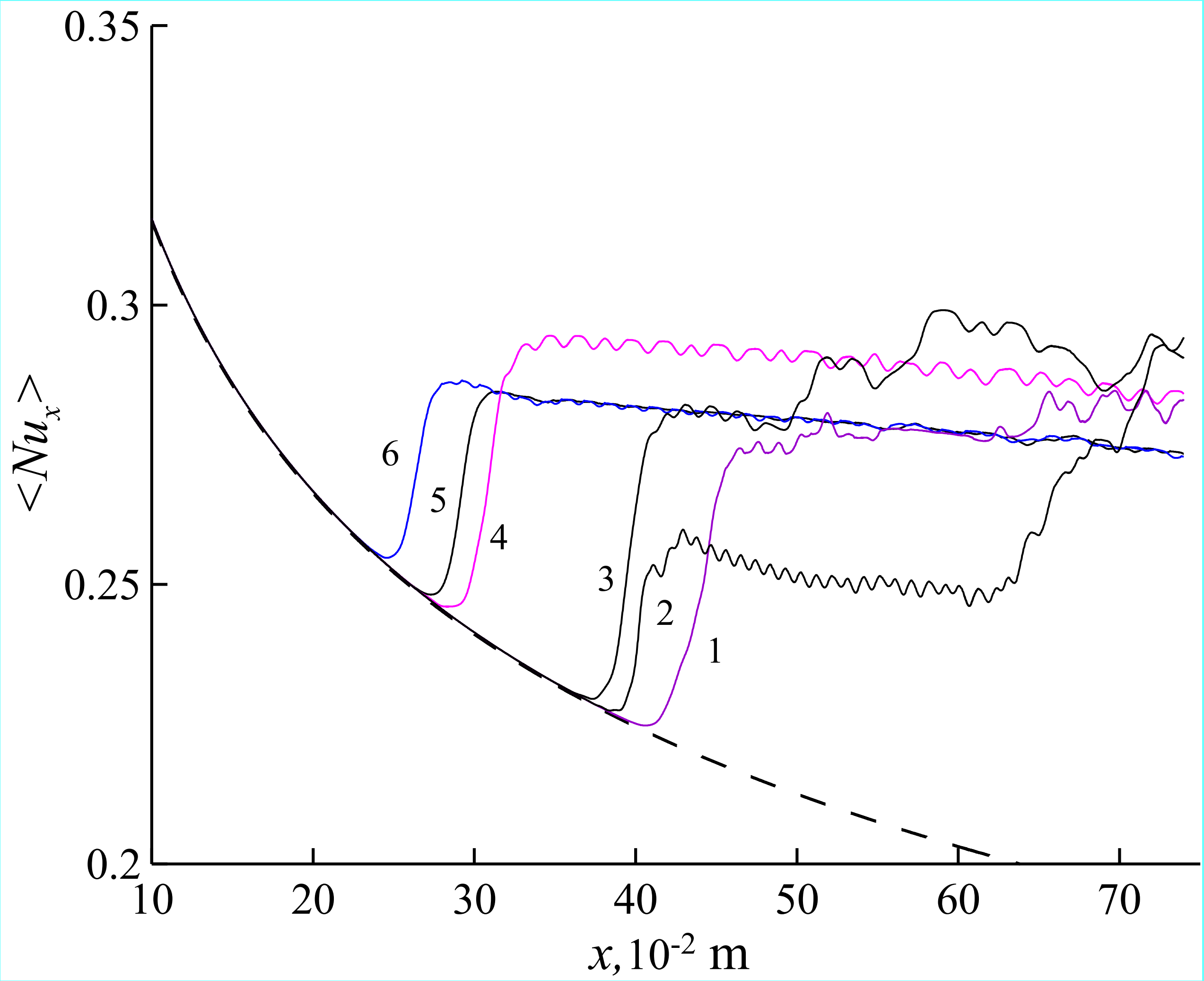

Dependence of time-averaged Nusselt number on coordinate;
1 – natural waves. Forced waves: 2–25 Hz, 3–3 Hz, 4–5 Hz, 5–18 Hz, and 6–9 Hz;
dashed line shows theoretical value for smooth film.

Wave effect on condensation

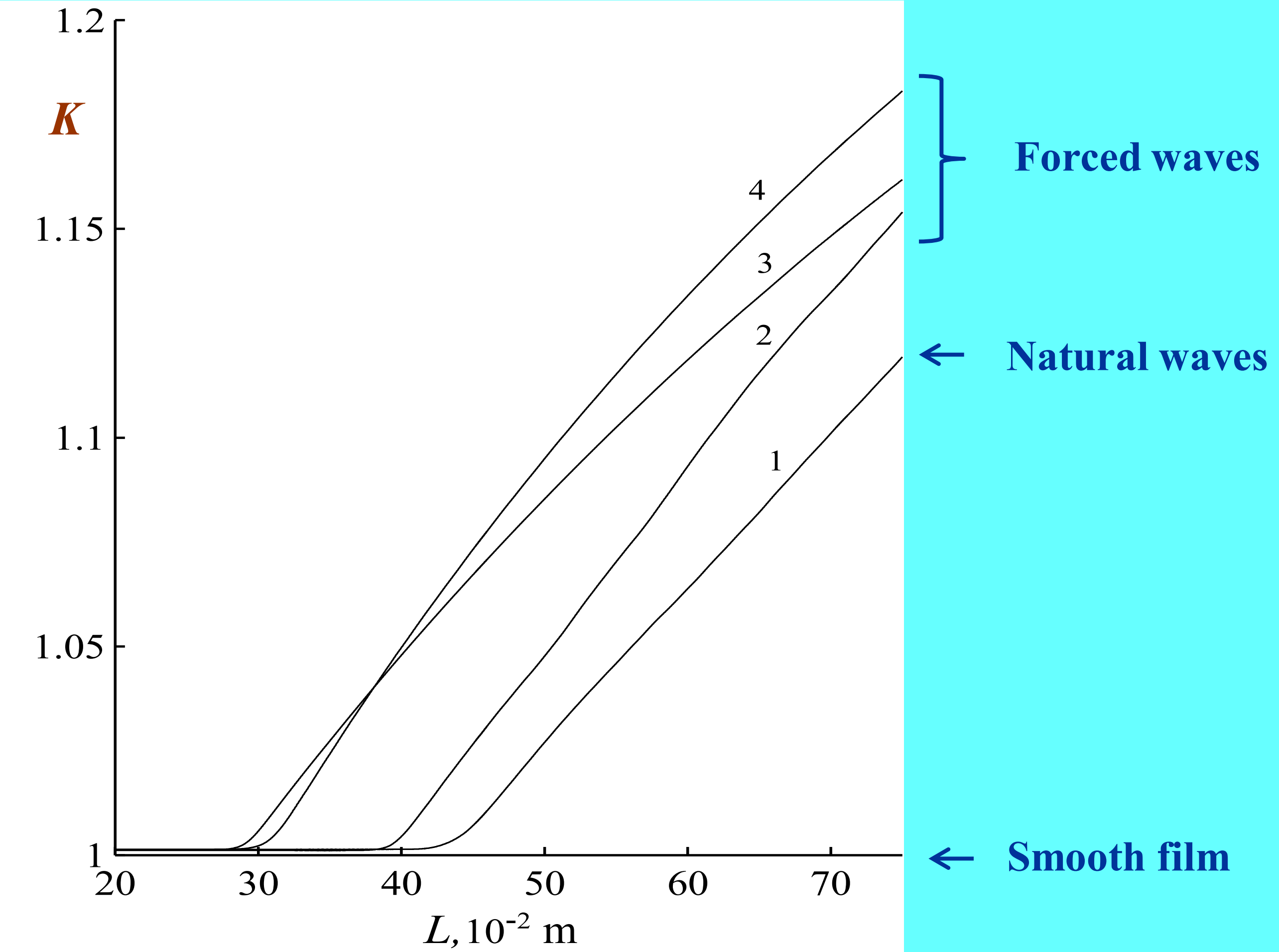

Dependence of the dimensionless integral coefficient of heat transfer enhancement *K* on the plate length *L*; 1 – natural waves.
Forced waves: 2 – 3 Hz, 3 –18 Hz, 4 – 5 Hz; *K* = 1 – smooth film.

Forced waves

Evaporation: $Re_m = 40$, $\varepsilon = 0.005$

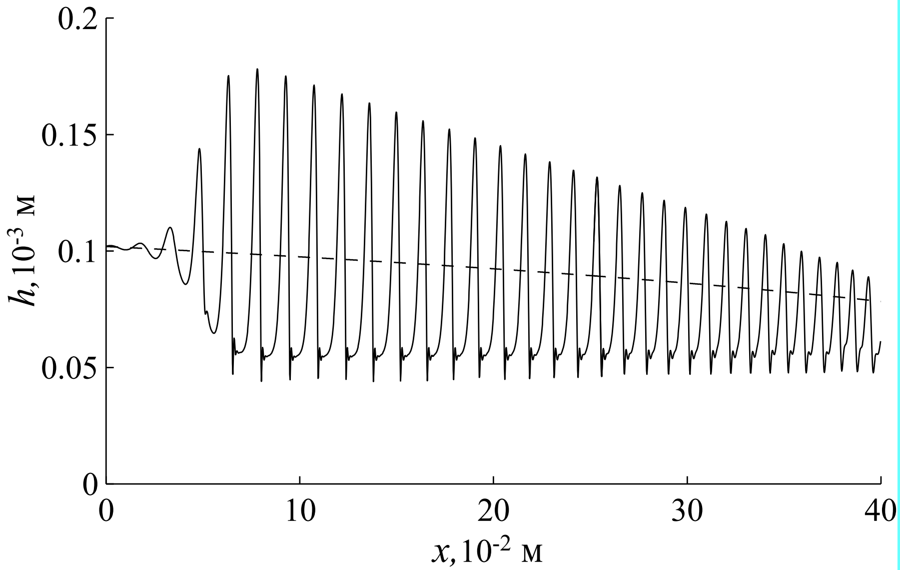

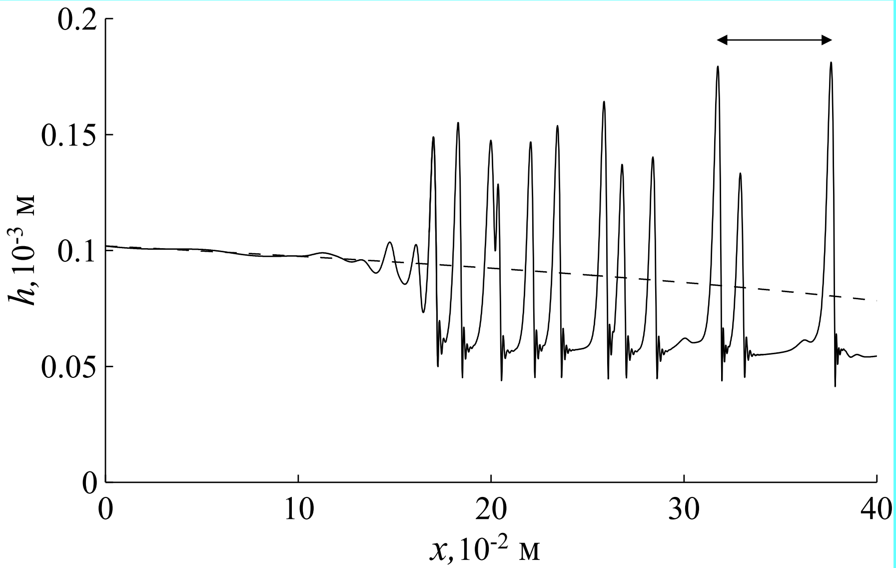

Waves with a frequency of 18 Hz;
dashed line corresponds to undisturbed film.

Amplitude of developed waves reduces with increasing distance from the inlet.

Waves with a frequency of 5 Hz.
Double-arrow section shows «wave length»;
dashed line corresponds to undisturbed film.

Absorption of additional peaks due to interaction.

Wave effect on evaporation

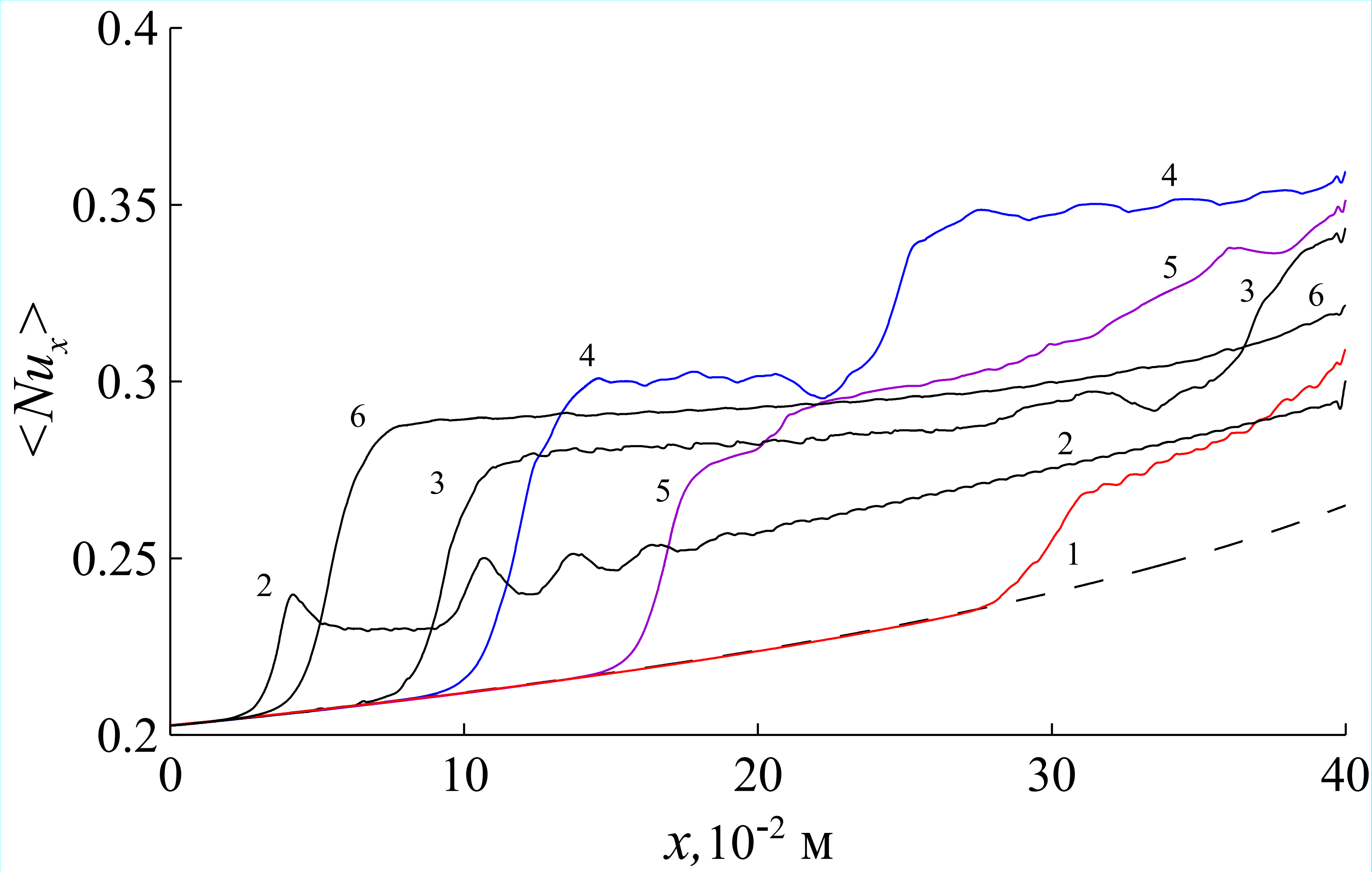

Dependence of time-averaged Nusselt number on coordinate;;
1 – natural waves. Forced waves: 2 – 30 Hz, 3 – 10 Hz, 4 – 8 Hz, 5 – 5 Hz, 6 – 18 Hz;
dashed line corresponds to theoretical value for smooth film.

Conclusion

The wave effect on condensation and evaporation was studied theoretically. It was shown that heat transfer enhancement by the waves occurs mainly due to a decrease in film thickness between the peaks.

It is demonstrated that using the method of superimposed periodic oscillations, one can enhance heat transfer within a certain frequency range as compared to the case of naturally occurring waves, and especially smooth film.

Instead of general conclusion: Problems and tasks related to film flows

1. Nonlinear three-dimensional waves
2. Stochastization of wavy regimes and transfer to turbulence
3. Interfacial turbulence
4. Interfacial stability in an annular two-phase flow
5. Mechanisms of drop entrainment in an annular two-phase flow
6. Countercurrent flow in regular packing. Maldistribution
7. Flooding and emulsification
8. Formation and stability of dry spots
9. Wave flow of rivulets and bridges
10. Wave effect on transfer processes
11. Condensation of vapor with non-condensable additions
12. Heat transfer in a liquid film will a local heat source
13. Stability and transfer processes in liquid films on rotating and moving bodies
14. Two-phase flow and heat transfer in capillary channels
15. Augmentation of transfer processes in film apparatuses
16. Nanofilms and nanofluids